

NATIONAL OCEAN SERVICE STELLAR CALIBRATION PROCEDURE

FOR THE LARGE FORMAT CAMERA

by

Karen Ann Theresa Podczasy

Report submitted to the Faculty of the

Virginia Polytechnic Institute and State University

in partial fulfillment of the requirements for the degree of

MASTER OF ENGINEERING

in

Civil Engineering

APPROVED:

---

S. Johnson, Chairman

---

L. Perry

---

J. Baker

June, 1984

Blacksburg, Virginia

NATIONAL OCEAN SERVICE STELLAR CALIBRATION PROCEDURE  
FOR THE LARGE FORMAT CAMERA

by

Karen Ann Theresa Podczasy

(ABSTRACT)

The Large Format Camera is a high resolution wide-angle mapping camera. It will be carried into orbit as a payload in the Shuttle Orbiter vehicle's cargo bay.

A mapping camera must be calibrated to determine precise values for its elements of interior orientation. The Large Format Camera was calibrated by the stellar method of camera calibration.

Descriptions of the procedure used by the National Ocean Service to calibrate the Large Format Camera are included.

## ACKNOWLEDGEMENTS

I wish to thank Lawrence Fritz of the National Ocean Service for allowing me to use their facilities while working on this paper. My especial thanks to Les Perry for his guidance and advice in preparing the Data Flow Diagrams and participation on my graduate committee; and William Golder for his patience and cooperation with me in answering my endless questions concerning all aspects of the calibration procedure. He often made special efforts to obtain necessary information for this paper. I also want to thank Dr. James Baker for participating as a member of my graduate committee; Dr. Steven Johnson for his advice on format and editing my report; and the Defense Mapping Agency for funding my education.

## TABLE OF CONTENTS

Title Page . . . . .	i
Abstract . . . . .	ii
Acknowledgements . . . . .	iii
List of Figures . . . . .	vi
List of Tables . . . . .	vii
1. Introduction . . . . .	1
1.1 Large Format Camera Characteristics . . . . .	3
1.2 Camera Calibration Definition . . . . .	8
1.3 Calibration Methods . . . . .	9
1.4 Objective and Scope . . . . .	11
2. Observation and Data Reduction Procedures . . . . .	13
2.1 Comparator Calibration . . . . .	13
2.2 Comparator Measurement Procedure . . . . .	14
2.3 Fiducial and Reseau Grid Calibration . . . . .	15
2.4 Field Procedure . . . . .	18
2.5 Preliminary Calculations . . . . .	19
2.6 Film Measurement . . . . .	21
2.7 Preliminary Data Reduction . . . . .	22
3. Camera Calibration Computer Programs . . . . .	25
3.1 Single Camera Orientation Program . . . . .	25
3.1.1 Coordinate Systems . . . . .	25
3.1.2 Corrections for Atmospheric Refraction and Aberration . . . . .	29
3.1.3 Corrections for Distortion and Nonperpendicularity . . . . .	31
3.1.4 Least Squares Observation Equations . . . . .	39
3.1.5 Least Squares Adjustment . . . . .	40
3.2 Multi-plate Camera System Calibration Program . . . . .	43
3.3 Flow Diagrams . . . . .	44
4. Calibration Results . . . . .	54
4.1 Application Equations . . . . .	54
4.2 Distortion Plots . . . . .	56

4.3 Systematic Distortion Plots . . . . .	60
5. Conclusions . . . . .	64
6. Summary . . . . .	66
Bibliography . . . . .	68
Appendix . . . . .	70

## LIST OF FIGURES

1.1	The Large Format Camera . . . . .	2
1.2	Large Format Camera Fiducial and Reseau System . . .	5
1.3	Large Format Camera Lens Cone and Magazine Layout . . .	7
3.1	Camera Orientation Parameters . . . . .	27
3.2	Perturbed Plate Coordinates . . . . .	32
3.3	Conrady Decentered Lens Distortion . . . . .	35
3.4	Combined Radial and Decentered Lens Distortion . . .	37
3.5	Nonperpendicularity of the Comparator Axis . . . . .	38
3.6	Overview of the Large Format Calibration Procedure . . .	47
3.7	Grid Calibration Process . . . . .	48
3.8	Grid Coordinate Transformation Process . . . . .	49
3.9	Preliminary Calculations . . . . .	50
3.10	Film Measurement . . . . .	51
3.11	Preliminary Data Reduction . . . . .	52
3.12	Camera Calibration . . . . .	53
4.1	Radial Symmetric Distortion Curve . . . . .	57
4.2	Transformed Radial Symmetric Distortion Curve . . . . .	58
4.3	Lens Decentering Distortion Curve . . . . .	59
4.4	Radial Symmetric Lens Distortion . . . . .	61
4.5	Lens Decentration Distortion . . . . .	62
4.6	Total Math Model of Systematic Distortion . . . . .	63
A.1	Large Format Camera Certificate of Calibration . . . . .	71
A.2	Fiducial and Magazine Reseau Numbering System . . . . .	72
A.3	Large Format Camera Calibration Parameters . . . . .	73
A.4	Large Format Camera Calibration Fiducial Coordinates . . . . .	74
A.5	Large Format Camera Magazine Reseau Coordinate System . . . . .	75
A.6	Star Images Measured on Each Plate . . . . .	84-85

## LIST OF TABLES

1.1	Large Format Camera Operational Parameters . . . . .	4
3.1	Large Format Camera Computers and Programs . . . . .	46
5.1	Design Requirements vs. Stellar Calibration Results . . . . .	65
A.1	Large Format Camera Magazine Réseau Coordinates . . . . .	76
A.2	Large Format Camera Calibration Parameters and Their Standard Errors . . . . .	77
A.3	Variance-covariance Matrix of Mean Camera Calibration Parameters . . . . .	78
A.4	Distortion Curve Data . . . . .	79-82

## 1. INTRODUCTION

The camera system is the most frequently used imaging system for the recording of data for photogrammetric measurements. When a camera is carried aloft in an aircraft or used in space to photograph the Earth, the moon, or other solar bodies, it is referred to as an aerial camera. One type of aerial camera is called a cartographic camera. It is designed specifically for use in photogrammetry to obtain the most accurate geometric data. The cartographic camera is employed in the production of maps.

Several factors have been dominant in the development of mapping cameras. One factor is that certain constant spatial relationships exist between the lens, the focal plane, and the fiducial markers. Also, for topographic mapping, photography is preferably taken with a wide angle camera so that a large base-height ratio is obtained. This enables a more accurate compilation of terrain relief.

Data requirements for topographic mapping include stereoscopic coverage for terrain-contour delineation, high image resolution for delineation of hydrographic and cultural features and high geometric integrity for correct location of all features.

One camera which possesses the requirements necessary to produce stereoscopic coverage adequate for topographic compilation is the Large Format Camera shown in Figure 1.1.



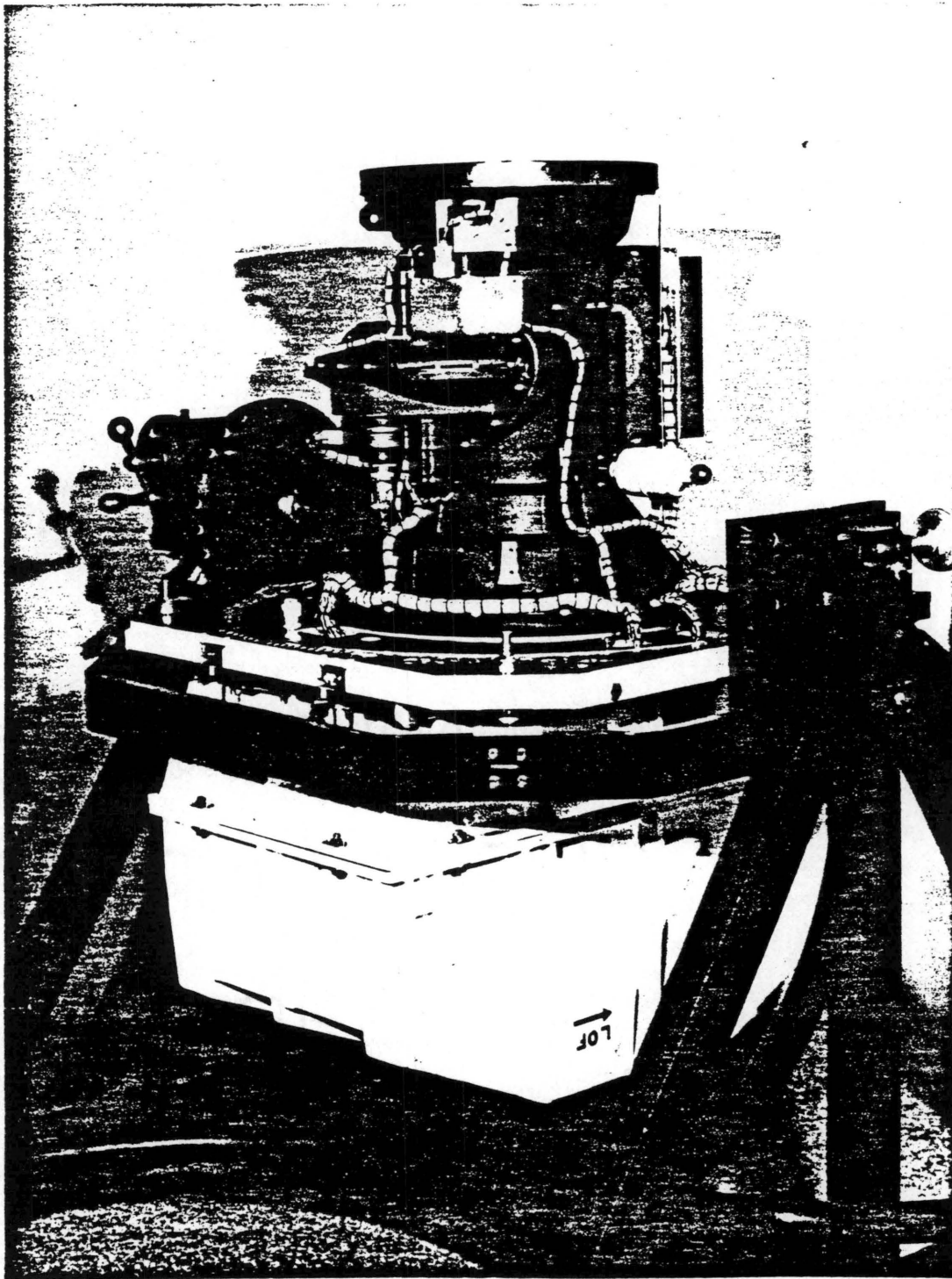


Figure 1.1 The Large Format Camera (NASA, 1979)

It was developed by NASA in response to an interest in the acquisition of a high-resolution wide-angle camera for mapping from a space environment.

The Large Format Camera is the major component of the Orbiter Camera Payload System which will be carried into Earth orbit as a payload in the Shuttle Orbiter vehicle's cargo bay. The Large Format Camera represents the first opportunity to acquire topographically-useful space photography of the Earth, from which planimetric detail and relief for 1:50,000-scale maps can be compiled in regions containing adequate geodetic control.

### 1.1 Large Format Camera Characteristics

Table 1.1 provides a summary of some of the design and operational parameters of the Large Format Camera. A description of some of the parameters is given in the following paragraphs.

The focal plane of the Large Format Camera's cartographic lens assembly is outlined by a metal frame with an opening which is 9 x 18 inches. As a key to image point location and mensuration, there is a total of 12 fixed fiducial references surrounding the format as shown in Figure 1.2. Subsets of the fiducials may be used to define the central or end 9"x 9" square areas of the format. These subsets permit the use of 9"x 9" portions of the photograph for measurement and use on standard photogrammetric

Table 1. Large Format Camera Operational Parameters  
(Mollberg, 1979)

Lens:	
Focal length	30.5 cm (12")
Aperture	f/6.0 (T/16)
Spectral range	400 to 900 nm
Distortion	10 m (average)
Shutter:	
Type	3 disc rotary intralens with capping blade
Speed range	4 to 32 msce
Setting	External command or AEC
Forward motion type	Translation of platen
Compensation: Range	11 to 41 mrad/sec
Camera internal pressure	2 psig
Film flattening	Vacuum
Image format	22.9 x 45.7 cm (9 x 18")
Forward overlap modes	10, 60, 70, and 80%
Base to height ratios	0.3 to 1.2
Filters:	
Antivignetting	Front of lens
Minus-haze	Intralens
Minus-blue	Intralens
Minimum cycle time	7 sec.
FOV:	
Along track	73.7° (ratio = 1.5 x H)
Across track	41.1° (ratio = 0.7 x H)
Film:	
Width	24.1 cm (9.5")
Roll length	1,220 m (4,000 ft.)
Exposures/roll	2,400
Electrical:	
Voltage	28 ± 4 Vdc
Power	273 watts (average)
Total flight weight	435.1 kg (959.2 lb.)
Altitude:	
Orbital	165 km min. (90 n. mi.)
Aircraft	19.8 km max. (65K ft.)

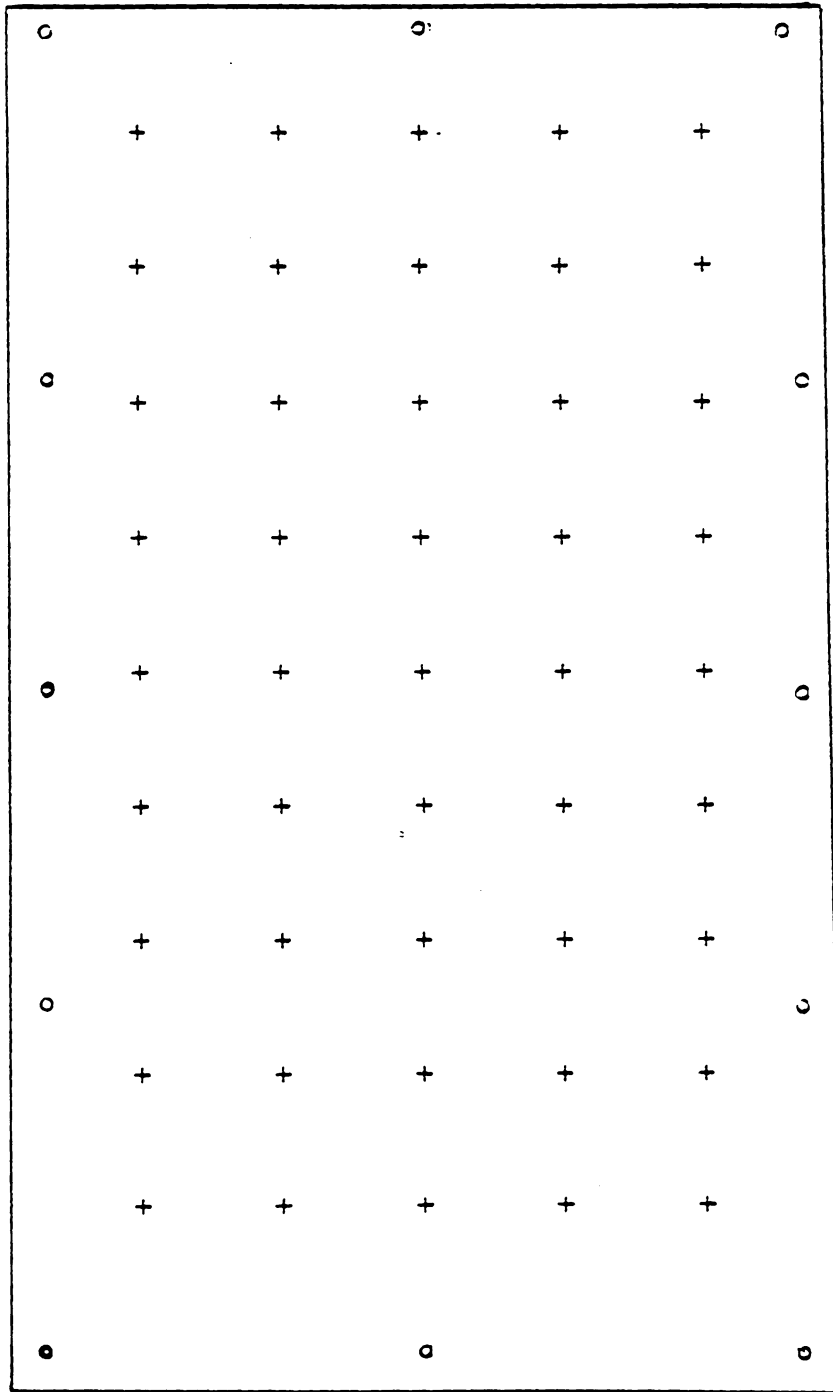


Figure 1.2 Large Format Camera Fiducial and Reseau System

instrumentation.

The Large Format Camera lens, shown in Figure 1.3, is composed of eight optical elements plus an antivignetting filter. A two-position filter changer is positioned at the lens' aperture. A minus haze and a minus blue filter are provided in the filter changer assembly and are selectable during flight by external command.

The between-the-lens rotary shutter is composed of three contrarotating disks and a capping blade. Shutter velocity is selected by either a programmed command or controlled by the output of automatic exposure control logic which is driven by a scene brightness sensor pointed at ground nadir. As the Large Format Camera is carried forward by the Orbiter, the exposure sensor examines a 1.8 degree spot at nadir and searches for the lowest brightness level over a period inversely proportional to altitude. After the data collection period, the result is used to control exposure over the next period, while new data is being sampled. By using the lowest brightness level to control exposure, the effects of clouds, specular reflection from water, and snow cover are removed from the exposure decision.

The camera magazine, also shown in Figure 1.3, contains lightweight dancer rollers on both the supply and takeup sides to accommodate the film unspooled during

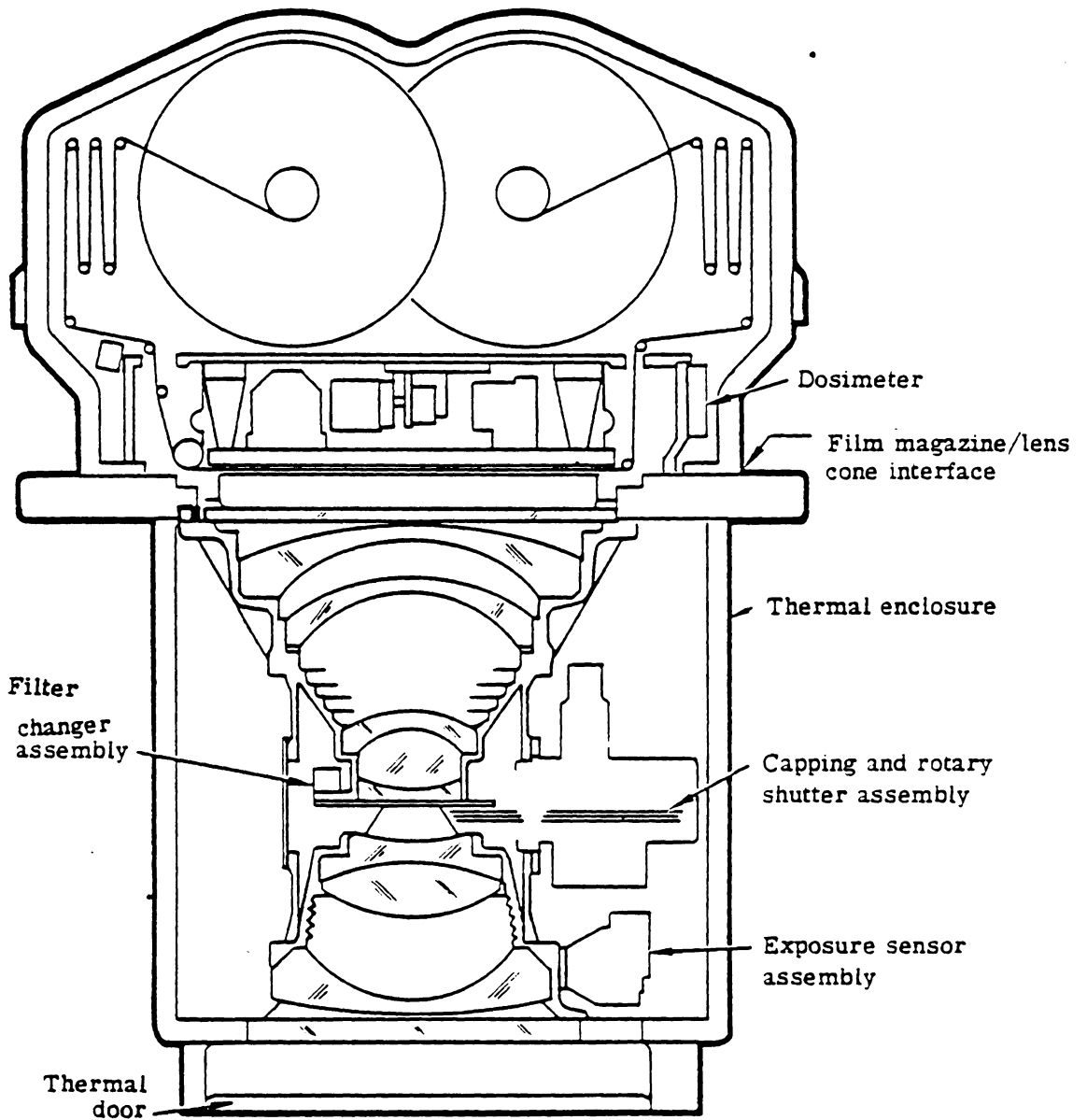


Figure 1.3 Large Format Camera Lens Cone and Magazine Layout (Itek, 1977)

camera cycle time. The platen is used to accomplish several functions. First, by means of a vacuum network, it flattens the film and holds it within the defined focal plane during image exposure. Second, while holding the film firmly in place, the platen translates in the opposite direction of flight to provide the necessary forward motion compensation during image exposure. The platen also contains a reseau at 5 cm intervals which is a fixed reference for the removal of film distortion. The reseau produces dot images provided by 0.05 mm holes in the platen, illuminated by light-emitting diodes from the rear of the platen. The reseau can be switched on or off by command.

## 1.2 Camera Calibration Definition

After a camera has been assembled by the manufacturer and prior to use, a camera must be calibrated to determine precise values for a number of camera constants. These constants are termed interior orientation parameters.

The calibration procedure involves reconstruction of the precise geometry of the bundle of rays that entered the camera at the instant of exposure from the two-dimensional measurement of points on the resulting photograph.

Depending on the quality of the camera, the interior orientation parameters which are calibrated may include the following:

1. Calibrated Focal Length - the distance measured along the optical axis from the rear nodal point of the lens to the plane of critical focus of a very distant object
2. Principal Point - the foot of the perpendicular from the interior perspective center to the plane of the photograph
3. Radial Symmetric Distortion - linear displacement of image points radially to or from the center of the image field, caused by the fact that objects at different angular distances from the lens axis undergo different magnifications
4. Decentered Lens Distortion - displacement of the image caused by errors made in assembling the lens so that the centers of curvature of the individual elements are not made to fall on a straight line.

### 1.3 Calibration Methods

The following list contains several methods of calibrating aerial mapping cameras.

1. Multicollimator (Laboratory)
2. Goniometer (Laboratory)
3. Stellar (Field)
4. In-flight (Field)

The basic differences between each are the selection of targets and methods of evaluating data.

The multicollimator calibrator uses the camera to be tested to photograph test targets placed in collimators at known angular separations. A collimator consists of a highly-corrected lens with a cross as the target mounted in its plane of infinity focus. All of the collimators



converge upward toward a central point. After the photographic plate is exposed and developed, the finished negative contains a row of target images along each diagonal, together with images of the fiducial marks in the camera focal plane. Measurements of the distances between each imaged cross are used to compute the following calibration parameters:

1. Equivalent focal length
2. Radial lens distortion
3. Tangential lens distortion
4. Location of the principal point

The resolving power of the lens at different field angles can be determined by an analysis of the resolution targets at each point along the diagonals.

The goniometer method of camera calibration consists of placing a graduated glass plate in the image plane of the camera. A goniometer is used to measure angles at the perspective center of the plate subtended by image points appearing on the plate. From these measurements, the focal length, distortion and location of the principal point can be calculated.

In the stellar method, the stars are used as targets. Film or glass plates are exposed at a camera station whose approximate latitude and longitude are known. The time of exposure is recorded. Under favorable atmospheric and lunar conditions, several hundred stars can be imaged on a single

exposure. The positions of the star images on the exposed emulsion are compared analytically with the theoretically correct image positions computed from the known(cataloged) astronomic positions. The differences between the measured and computed positions of the star images then represent the lens distortions. The focal length, location of the principal point and distortions are determined as functions of the positions of the stars, the camera perspective center, and the star images. The mathematical models for distortions are introduced directly into the photogrammetric projective equations and recovered simultaneously with the interior orientation parameters in a least squares adjustment.

A fourth method of calibrating a camera is in-flight calibration. The camera is mounted in an airplane or space vehicle. Exposures are taken as the vehicle is flown over a three-dimensional control range. The data can be reduced using analytical methods from which the interior and exterior parameters are determined.

#### 1.4 Objective and Scope

The objective of this paper is to describe the calibration procedure used by the National Ocean Service to calibrate the Large Format Camera. The Large Format Camera was calibrated using the stellar method. The stellar method was chosen because it provides the most definitive and

comprehensive calibration available for metric cameras to date. A preliminary step in preparation for this paper involved the representation of the Large Format Camera calibration procedure in the form of a Flow Diagram. The Flow Diagram was developed by determining the flow of data through the many processes of the calibration procedure. It is included at the end of Chapter 3.

The calibration is described in two parts. The procedures leading up to the reduction of the measured star data are given in Chapter 2. Chapter 3 contains descriptions of the two major computer programs used to process the data to obtain the calibration parameters.

Chapter 4 contains some of the diagnostic plots included in the Large Format Camera Calibration Certificate. The remaining data from the certificate is presented in the Appendix.

## 2. OBSERVATION AND DATA REDUCTION PROCEDURES

The order in which the procedures are presented in this chapter does not necessarily imply the order in which they are performed. For example, calibration of the comparator to be used for measurements must be done before the exposed film can be measured. However, the field procedure which involves exposing the film to the stars can be done before the comparator calibration.

### 2.1 Comparator Calibration

The images of the stars on the film are measured using a two-coordinate comparator. The coordinates of the star, fiducial, and reseau images must be measured with extremely high accuracy. This accuracy depends on the measuring equipment and the measuring procedure.

The measuring equipment consists of the measuring comparator and the peripheral equipment for recording the measurements. In order to achieve the maximum accuracy in the mensuration process, the comparator itself must be calibrated. Comparators have mechanical imperfections which result in the creation of systematic measuring errors. These errors can be modeled mathematically and removed.

A comparator calibration procedure requires the use of a precision glass grid plate. The grid plate was provided by the National Ocean Service. The plate was marked by

well-defined gridline intersections symmetrically spaced 5 cm apart. The grid was placed in the comparator and twenty-five grid intersections were measured. From the x and y coordinates of the intersections, several comparator calibration parameters were determined.

The calibrated grid positions are defined in an orthogonal coordinate system. The comparator measurement coordinate system is nonorthogonal due to inherent mechanical limitations. Thus, the x and y scale factors and angle of non-orthogonality were found between the two systems. There are also a variety of nonlinear systematic errors that are present in the comparator. The nonlinear errors were removed by applying a fourth degree polynomial to the measurement of each axis. The linear and nonlinear comparator calibration parameters must be removed from all of the measurements of the camera calibration procedure.

## 2.2 Comparator Measurement Procedure

All measurements of the Large Format Camera calibration procedure were made using a precision Laser Mann Automatic Stellar Comparator. The comparator is equipped with an on-line PDP-8L computer that is pre-programmed to automatically drive the comparator stage to the desired measurement points. The comparator employs a density centroid correlation technique for automatic measurement of high-contrast symmetrical images, such as dots.

In order for the comparator to find each point, the program it uses requires initial approximations of the coordinates for the points. These coordinates are set up based on the known distance between the points. Also, since the coordinate system of the approximate coordinates is not coincident with the comparator coordinate system, a transformation containing rotation and translation values is needed between these two systems. Thus the comparator program takes the approximated coordinates, applies the transformation parameters, and uses the translated coordinates to drive automatically to each point.

When a point is located, the image will not be centered because the comparator is using only approximated coordinates. At this time the image can be centered and measured either manually or automatically, depending on the symmetry of the image.

### 2.3 Fiducial and Reseau Grid Calibration

A total of three grids were calibrated as part of the Large Format Camera calibration. The first two are the fiducial grid and magazine reseau grid. A third grid called the focal plane calibration fixture reseau was also calibrated. The focal plane calibration fixture reseau is a grid work of 285 crosses at 2 cm spacing etched on a glass plate. It was exposed along with the stars instead of the magazine reseau. The focal plane calibration fixture

reseau was easier to handle because it weighs much less than the magazine reseau.

The calibration procedure for each type of grid is basically the same and will only be described for the fiducials. However, any differences in procedure for either reseau grid will be noted.

Usually one 10 x 10 inch microflat glass plate is sufficient to cover the format of a cartographic camera. However, three glass plates were required to cover the 9 x 18 inch format of the Large Format Camera as 10 x 9 inch microflat plates are exorbitantly expensive. Each of the grids was exposed on Kodak type 131-01 high speed holographic plates measuring 10 x 10 inches. One glass plate was exposed to the upper (top) third of the fiducial format, a second glass plate to the middle third, and a third glass plate to the lower (bottom) third of the format. Due to the size of the glass plates and for geometric strength for the grid calibration, there was some overlap between them. The three exposed glass plates will be referred to as top, middle, and bottom plates. Each section of the fiducials was exposed twice, producing six exposed glass plates.

Since the magazine reseau produces dot images, they were measured automatically. However, the fiducials and fixture reseau were measured manually.

Each image was measured with three pointings in each of four 90 degree positions for each of the six photographic plates. This produced a total of twenty-four independent groups of measurements; eight for the top plates, eight for the middle plates and eight for the bottom plates.

The comparator calibration parameters were applied to all the measurements. Each of the twenty-four groups were then rotated and translated(no scaling) to a common orientation system. The orientation system was a set of ideal grid coordinates in the desired final coordinate system orientation. The ideal grid coordinates were set up based on the nominal spacing between them. The eight groups of measurements for the top plate were meaned, as well as the eight groups for the middle and bottom plates. The group of meaned coordinates for the top plate were rotated, translated and scaled to the coordinates of the middle plate. The grid coordinates in the overlap between the top and middle plates were used for this transformation. The same procedure was used to transform the bottom plate coordinates to the middle plate. Duplicate coordinates from the overlap areas of the plates were meaned. These meaned coordinates together with the middle plate coordinates and transformed top and bottom plate coordinates provided a provisional set of calibrated grid coordinates.

Finally, each of the original twenty-four groups of



grid coordinates were rotated, translated and scaled to this set of provisional calibrated grid coordinates. All duplicate coordinates were meant to produce the final calibrated grid coordinates.

#### 2.4 Field Procedure

The stellar exposure site for the Large Format Camera was the National Ocean Service camera stellar calibration observatory located in Cloudcroft, New Mexico. Preparations were made to the building before the Large Format Camera was shipped to the site. These preparations included the construction of an isolation fixture to support an external capping shutter and a special stable mount to support the oversize Large Format Camera during the stellar exposures.

Once the camera was received at Cloudcroft, it was mounted on the platform and the external capping shutter was installed over the lens cone. A dark cloth shroud was placed around this setup to prevent exposure from stray light during film loading. Thermistor probes were used to remotely monitor temperatures of the focal plane calibration fixture, the ambient air underneath the shroud and the cone base of the Large Format Camera. In addition, the exposures were scheduled for nights which were cloud-free, haze-free and moonless.

Plus-X Aerographic film was used for the exposures.

The film was pre-exposed to dim light in the darkroom to make the film more sensitive to the light from the stars. A vacuum network was used to flatten the film against the focal plane calibration fixture and hold it in the focal plane during the image exposure.

Operation of the capping shutter was controlled by a paper-tape-fed programmer unit which was interfaced with a precise timing unit. Greenwich Mean Time and all capping shutter commands and responses were recorded on a time tape.

The film was exposed first to the fiducials and then to the stars. Exposures were made over an extended period of time so that the motion of the earth, rotating on its axis, produced star trails on the film. For each exposure the camera was fixed into a position pointed at the zenith. A total of four exposures were taken, rotating the camera 90 degrees about its zenith for each succeeding exposure. Multiple exposures are necessary to minimize random errors of position. These errors result from variations in film unflatness and emulsion shifts.

## 2.5 Preliminary Calculations

The purpose of the preliminary calculations was to prepare the data from the Field Procedure in a form suitable for use in the computational procedures. This includes identification of ten well-distributed stars on the film and preparation of star catalog data for the

identified stars.

A computer program is used to locate stars within a specified area. The program utilizes the station position and Greenwich Mean Times to find stars located in the approximate field of view of the camera. The program assumes a zenith exposure from the latitude and longitude of the calibration site and a sidereal time corresponding to the midpoint of each exposure trail. The stars are chosen based on their right ascension, declination, and magnitude. The x and y coordinates for each star meeting the requirements were printed out. These stars were plotted on a chart to the scale of the photographic plate. The chart was laid over the film and rotated until the stars on the chart coincided with the stars on the film. Ten well-distributed stars were identified and marked on the film, and assigned identification numbers.

The right ascensions and declinations for the ten pre-selected stars were saved to be used in the Preliminary Data Reduction. They were used to obtain a preliminary interior and exterior camera orientation. A preliminary orientation was required for computer identification of the remaining catalogued star images on the plate.

To compute the exact position of each star at each exposure time, a set of parameters for each time including local sidereal time and updating parameters are necessary.

Using the station position, the date of observation and Greenwich Mean Time, a computer program computes the local sidereal times and updating parameters.

## 2.6 Film Measurement

The stellar film was also measured on the Laser MANN Automatic Stellar comparator. The stars were measured in three groups. The first group consisted of the ten pre-selected stars and all the fiducials. This group was called the Pre-Set. The procedure was to measure each star and record its x and y comparator coordinates. Then a minimum of four reseau points were measured around the star and their x and y comparator coordinates recorded.

To measure the second and third groups, the film was divided into eight sections so that the entire piece of film was not read in one session. According to Bush(1973), an operator's body heat causes an unacceptable amount of error in the comparator after two to three hours of measuring. The measurement of the entire piece of film would have taken at least eight hours.

The second group of measurements consisted of fiducials, reseau points and stars. The star images were measured by choosing at least one star trail(5 star images) within a "box" formed by reseau points. This set of measurements was called the A set.

When the A set was completed, the film was rotated 180

degrees and measurements were repeated to form the B set. This time, using the coordinates from the A set, the comparator was able to automatically drive to the stars as well as the reseau points. This was done so that the same stars were measured for the B set as for the A set. According to Fritz(1976), the second set of measurements is necessary to nullify operator pointing biases and statistically improve the final result through redundant observations.

## 2.7 Preliminary Data Reduction

The initial step was to refine the Pre-set coordinates by applying comparator calibration corrections to the measurements and transform them to the camera fiducial coordinate system.

Each of the A and B set measurements were refined by applying comparator calibration corrections. The eight sets of measurements for the A and B sets were transformed (linear affine) to the calibrated fixture reseau coordinate system. This was accomplished by first locating all of the reseau points within a pre-determined distance of each star image. The measured coordinates for these reseau points were used to determine transformation parameters between the measured and calibrated reseau coordinates. These transformation parameters were applied to the star coordinates. The A and B set measurements were then

measured and transformed(rotation and translation only) to the camera fiducial system.

The Pre-Set was used, along with the station latitude, to determine the apparent direction of the stars' path across the film. It was also used to compute a first approximation to camera orientation and approximate right ascensions and declinations were used as the basis for a search through the star catalog to find the actual identity and celestial coordinates of the stars.

In order to determine a first approximation to the camera orientation, the true positions of the photographed stars at the instant of exposure were needed. Star catalogs contain coordinates for the stars for epoch 1950.0. Because of long-term changes in the direction of the earth's axis and motion of the stars themselves, their celestial coordinates will have changed between epoch 1950.0 and the time of observation. Thus it is necessary to update the star position to the beginning of the Besselian year nearest the day of observation and then to the time of observation itself. The position of each star after updating must be adjusted for the effects of diurnal aberration and refraction. Then the standard coordinates for each star position are computed from the updated and corrected celestial coordinates. After all of these operations are completed, the plate constant method

described by Bush(1973), is employed to compute the camera orientation.

### 3. CAMERA CALIBRATION COMPUTER PROGRAMS

The two major computer programs of the National Ocean Service calibration procedure are the Single Camera Orientation program and the Multiple Camera System Calibration program. The math model used in the Single Camera Orientation program is described in the following section. The third section deals with the Multiple Camera System Calibration program.

#### 3.1 Single Camera Orientation Program

The Single Camera Orientation program is based on a mathematical model which simulates a camera and its orientation in inertial space. The computer program processes the comparator-measured refined coordinates of the star images on film along with directional coordinates of the stars and uses a least-squares technique to estimate camera orientation parameters. For complete derivations of equations presented in the following sections see Slama(1976).

##### 3.1.1 Coordinate Systems

The calibration parameters to be determined include the calibrated focal length, the principal point coordinates, and the radial symmetric and decentering lens distortion model coefficients. Also, the exterior



orientation of the camera must be determined. Therefore, the parameters of these orientations and the coordinate systems to which they relate must be defined.

The interior orientation deals solely with the camera coordinate system, relating the principal point and focal length to that system. The exterior orientation must relate the camera coordinate system to some fixed exterior coordinate system.

The relationship between an exterior or spatial coordinate system and its corresponding camera coordinate system is shown graphically in Figure 3.1.

The geocentric coordinate system was chosen as the object space coordinate system with the right ascension-declination reference system as the coordinates. These coordinates are transformed to a rectangular coordinate system where the celestial sphere is projected onto a plane tangent to the sphere at the observer's zenith. On the plane, the X-axis is positive toward the north and the Y-axis is positive toward the east. The third axis is through the zenith.

The rotation matrices relating the two coordinate systems are:

$$R_{\alpha} = \begin{bmatrix} \cos\alpha & 0 & -\sin\alpha \\ 0 & 1 & 0 \\ \sin\alpha & 0 & \cos\alpha \end{bmatrix}$$

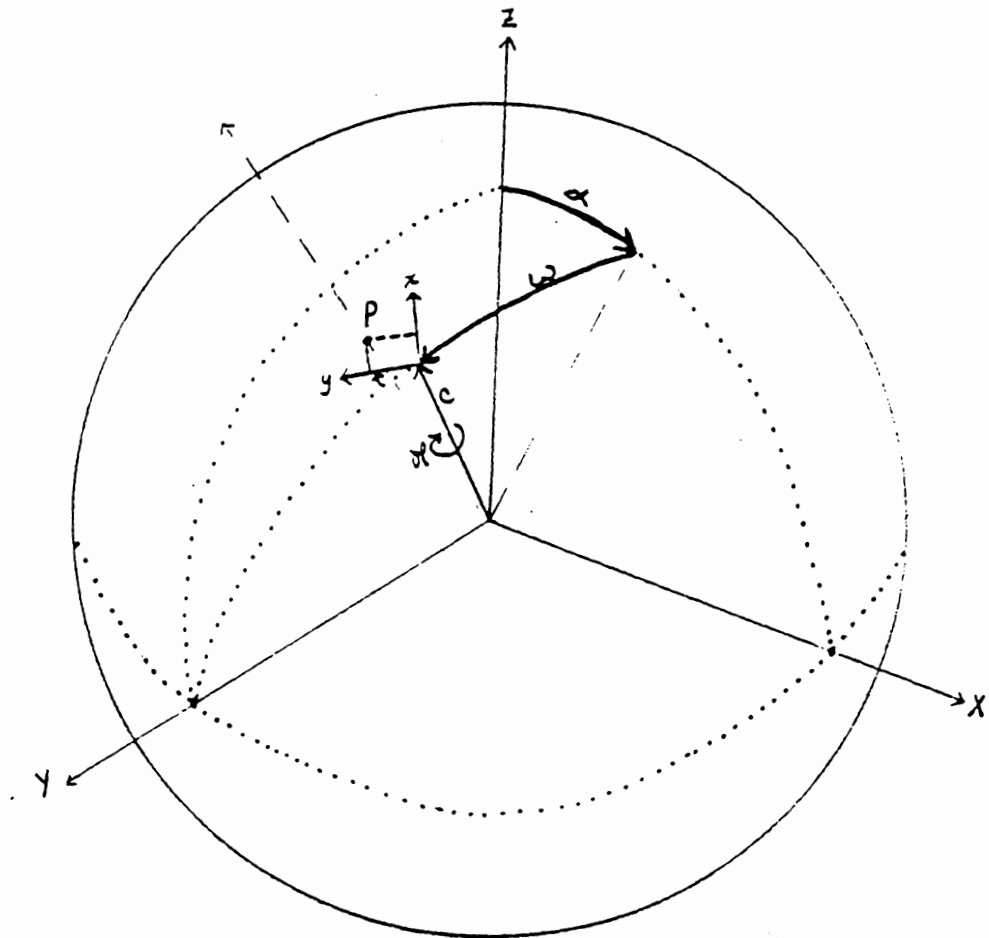


Figure 3.1 Camera Orientation Angles (Slama, 1972)

$$R_{\omega} = \begin{bmatrix} 1 & 0 & 0 \\ 0 & \cos \omega & -\sin \omega \\ 0 & \sin \omega & \cos \omega \end{bmatrix}$$

$$R_{\mathcal{K}} = \begin{bmatrix} -1 & 0 & 0 \\ 0 & 1 & 0 \\ 0 & 0 & 1 \end{bmatrix} \begin{bmatrix} \cos \mathcal{K} & \sin \mathcal{K} & 0 \\ -\sin \mathcal{K} & \cos \mathcal{K} & 0 \\ 0 & 0 & 1 \end{bmatrix}$$

$$R_{\mathcal{A}} = \begin{bmatrix} -\cos \mathcal{A} & -\sin \mathcal{A} & 0 \\ -\sin \mathcal{A} & \cos \mathcal{A} & 0 \\ 0 & 0 & 1 \end{bmatrix}$$

The matrices ( $R_{\mathcal{K}}, R_{\omega}, R_{\mathcal{A}}$ ) are multiplied together to form the orientation matrix  $M$  relating the spatial and photograph coordinate systems.

$$M = \begin{bmatrix} -\cos \mathcal{A} \cos \mathcal{K} + \sin \mathcal{A} \sin \omega \sin \mathcal{K} & -\cos \omega \sin \mathcal{K} & \sin \mathcal{A} \cos \mathcal{K} + \cos \mathcal{A} \sin \omega \sin \mathcal{K} \\ -\cos \mathcal{A} \sin \mathcal{K} - \sin \mathcal{A} \sin \omega \cos \mathcal{K} & \cos \omega \cos \mathcal{K} & \sin \mathcal{A} \sin \mathcal{K} - \cos \mathcal{A} \sin \omega \cos \mathcal{K} \\ \sin \mathcal{A} \cos \omega & \sin \omega & \cos \mathcal{A} \cos \omega \end{bmatrix}$$

The transformation from spatial to image coordinates is

$$\begin{bmatrix} x \\ y \\ c \end{bmatrix} = (1/\mu) M \begin{bmatrix} X \\ Y \\ Z \end{bmatrix} \quad (3.1)$$

where  $X, Y, Z$  are the spatial coordinates (updated star

catalog coordinates),  $x$  and  $y$  are the measured image coordinates,  $(1/\mu)$  is a scale factor, and  $c$  is the focal length.

The transformation from spatial to image coordinates can be written without the proportionality factor as

$$\begin{bmatrix} m \\ n \\ q \end{bmatrix} = M \begin{bmatrix} X \\ Y \\ Z \end{bmatrix} .$$

### 3.1.2 Correction for Atmospheric Refraction and Aberration

As the light from an observed celestial body passes through the earth's atmosphere, the variation of air density along the path causes a continuous change in the direction of propagation. This change in direction of the light ray is termed refraction. The general affect is that light rays are bent downward; thus the celestial body appears to be at a higher altitude than it is in reality. It is therefore necessary to eliminate from the observations the effects of the atmosphere.

The expression used to compute the atmospheric refraction is

$$\epsilon'' = T^{1/2} W (\tau_1 \tan \beta / 2 + \tau_2 \tan^3 \beta / 2 + \tau_3 \tan^5 \beta / 2 + \tau_4 \tan^7 \beta / 2)$$

where

$\Upsilon = T/T_0$  with  $T$  as station temperature and  $T_0$  as standard temperature

$$W = P^*/T^2$$

$P^* = P/P_0$  with  $P$  as station pressure and  $P_0$  as standard pressure

$\beta =$  a function of weather parameters and observed zenith distance of the object given by

$$\tan \beta = \frac{T^{1/2}}{\delta} \tan z$$

where  $\delta = 8.7137$ .

The coefficients  $\Upsilon_i$  are:

$$\Upsilon_1 = 1050.6103,$$

$$\Upsilon_2 = 706.11502,$$

$$\Upsilon_3 = 262.06086,$$

$$\Upsilon_4 = 142.67293.$$

The star positions must also be corrected for diurnal aberration. It results from the daily motion of the observer due to the rotation of the earth about its axis.

The equations used to compute the displacement (in seconds of arc) are:

$$\Delta \alpha = 0.320 \cos \varnothing \sin H \sec$$

$$\Delta \delta = 0.320 \cos \varnothing \sin H \sin$$

where

$\varnothing$  = the angle measured from the celestial equator to the observer's zenith

H = hour angle

$\delta$  = declination of star

These displacements are added to the input coordinates (apparent places) to obtain the corrected coordinates.

### 3.1.3 Corrections for Distortion and Nonperpendicularity

The plate measurements must be corrected for two types of distortion: 1) radial symmetric and 2) decentered lens distortion. Both of these distortions are shown in Figure 3.2. These distortions result in a physical displacement of the resulting image from its ideal projective position.

The equation which expresses the radial symmetric distortion is

$$\Delta R = K_1 d^3 + K_2 d^5 + K_3 d^7 \quad (3.2)$$

where

$K_i$  = unknown coefficients to be determined in the calibration

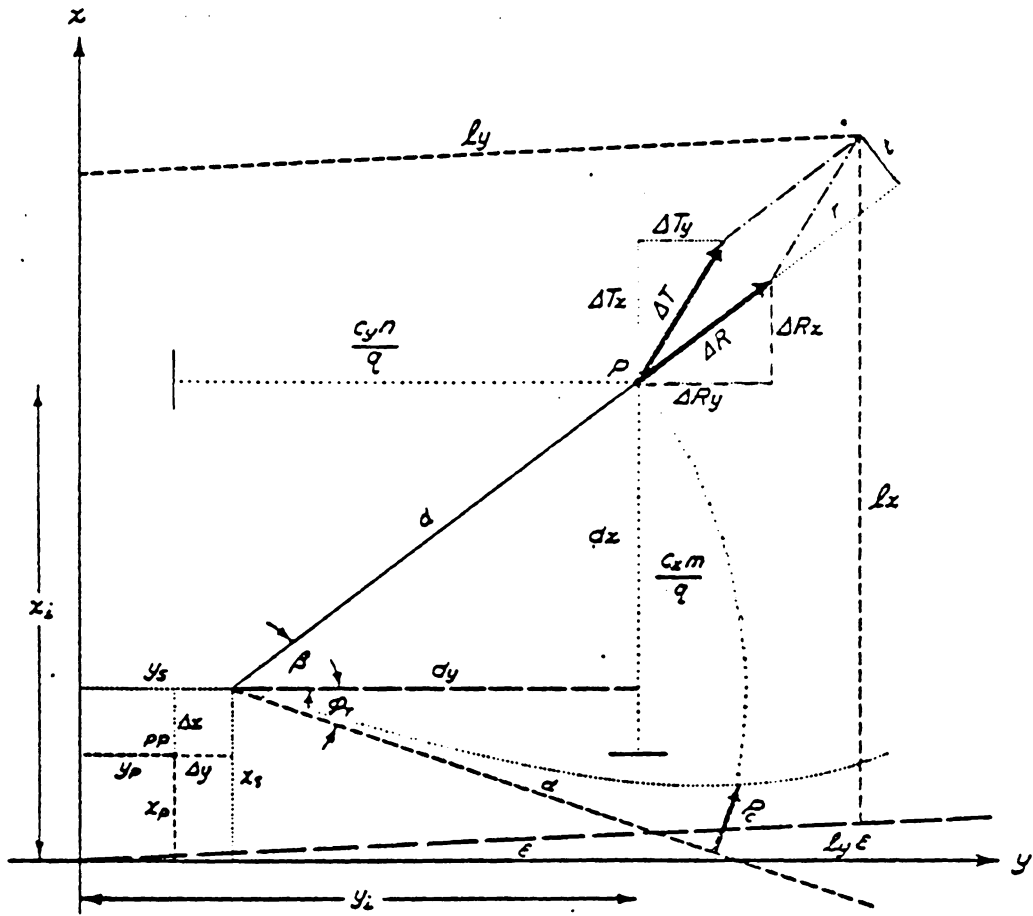


Figure 3.2 Perturbed Plate Coordinates (Slama, 1972)

$d$  = the radial distance from the point of symmetry to the distortion profile.

The  $x$  and  $y$  components of the radial symmetric distortion are

$$\Delta R_x = \frac{R}{d}(x_i - x_s) \quad (3.3)$$

$$\Delta R_y = \frac{R}{d}(y_i - y_s) \quad (3.4)$$

where

$x_s, y_s$  = coordinates of the principal point of symmetry.

The expressions for displacements resulting from decentrations of lens elements are

$$r = 3p_3 V^2 \cos \chi \quad (3.5)$$

$$t = p_3 V^2 \sin \chi \quad (3.6)$$

where

$V$  = half angle of view of the image

$p_3$  = constant peculiar to the lens system

$\chi$  = angle indicating the orientation of the image relative to the direction of decentration

$r$  = positive away from the origin along the radial line of the field

$t$  = perpendicular to the radial line.



The distortion profile,  $p_3V^2$ , is given by the polynomial  $K_4d^2 + K_5d^4$ .

From Figure 3.3, using  $\lambda = \varnothing_T + \beta - 90^\circ$ , the equations 3.5 and 3.6 are written in terms of  $\varnothing_T$  and  $\beta$  as

$$r = 3p_3V^2 \sin(\varnothing_T + \beta) \quad (3.7)$$

$$t = -p_3V^2 \cos(\varnothing_T + \beta) \quad (3.8)$$

Using expressions 3.7 and 3.8 and rotating the  $r, t$  system through an angle  $\beta - 90^\circ$ , the  $x$  and  $y$  components of the decentered lens distortion  $\Delta T$  in the plate system are

$$\begin{aligned} T_x &= (x_i - x_s)(K_4 + K_5d^2) \left( \frac{3dx^2 + dy^2}{dx} \cos\varnothing_T + 2dy \sin\varnothing_T \right) \\ &= (x_i - x_s)D_x \end{aligned} \quad (3.9)$$

$$\begin{aligned} T_y &= (y_i - y_s)(K_4 + K_5d^2) \left( \frac{3dx^2 + dy^2}{dy} \sin\varnothing_T + 2dx \cos\varnothing_T \right) \\ &= (y_i - y_s)D_y \end{aligned} \quad (3.10)$$

where

$$\cos\beta = \frac{dy}{d}$$

$$\sin\beta = \frac{dx}{d}$$

$$dx = (x_i - x_s)$$

$$dy = (y_i - y_s)$$

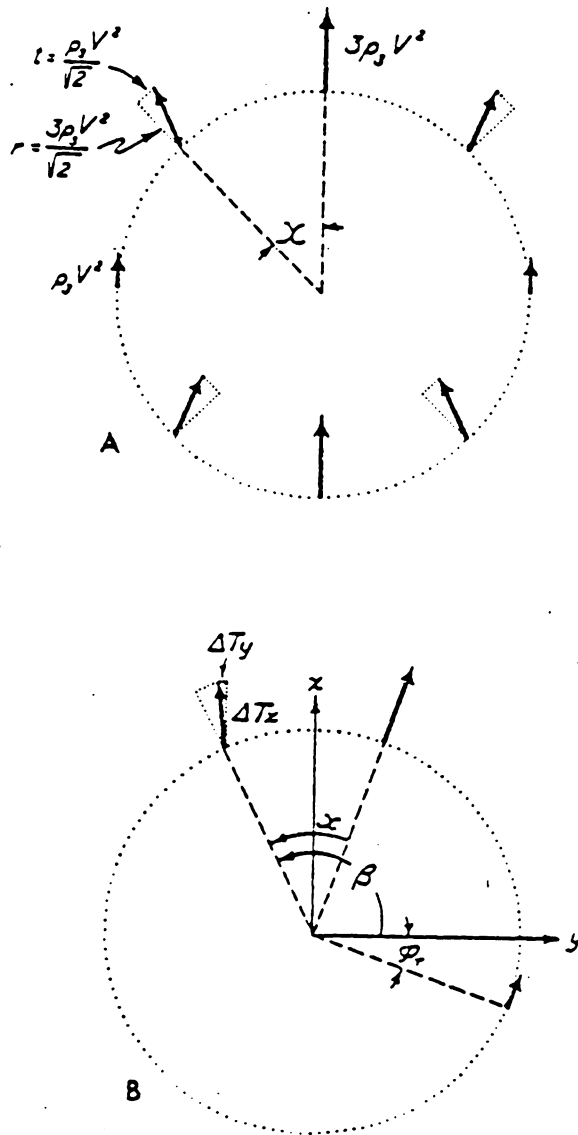


Figure 3.3 Conrady Decentered Lens Distortion (Slama, 1972)

Therefore, the components  $(\delta_x, \delta_y)$  of the displacements resulting from a combination of both radial and lens decentering distortion evaluated at a distance  $d$  from the point of origin of the distortion profiles shown in Figure 3.4 are

$$\delta_x = \Delta R_x + \Delta T_x = (x_i - x_s) \left( \frac{\Delta R}{d} + D_x \right) \quad (3.11)$$

$$\delta_y = \Delta R_y + \Delta T_y = (y_i - y_s) \left( \frac{\Delta R}{d} + D_y \right) \quad (3.12)$$

where the coordinates of the displaced image are given by

$$\bar{x}_i = x_i + \delta_x \quad (3.13)$$

$$\bar{y}_i = y_i + \delta_y \quad (3.14)$$

Two additional image deformations which are accounted for are a differential scale change  $(C_x, C_y)$  along the  $x$  and  $y$  plate axis  $(\epsilon)$  as depicted in Figure 3.5. The total effect of these two deformations in matrix form is given by

$$\begin{bmatrix} x_i \\ y_i \\ C_x \end{bmatrix} = \begin{bmatrix} 1 & (-C_y/C_x) & 0 \\ 0 & C_x/C_y & 0 \\ 0 & 0 & 1 \end{bmatrix} \begin{bmatrix} \bar{x}_i \\ \bar{y}_i \\ C \end{bmatrix} \quad (3.15)$$

The complete expressions for the projective transformation from object space (star coordinates) to image

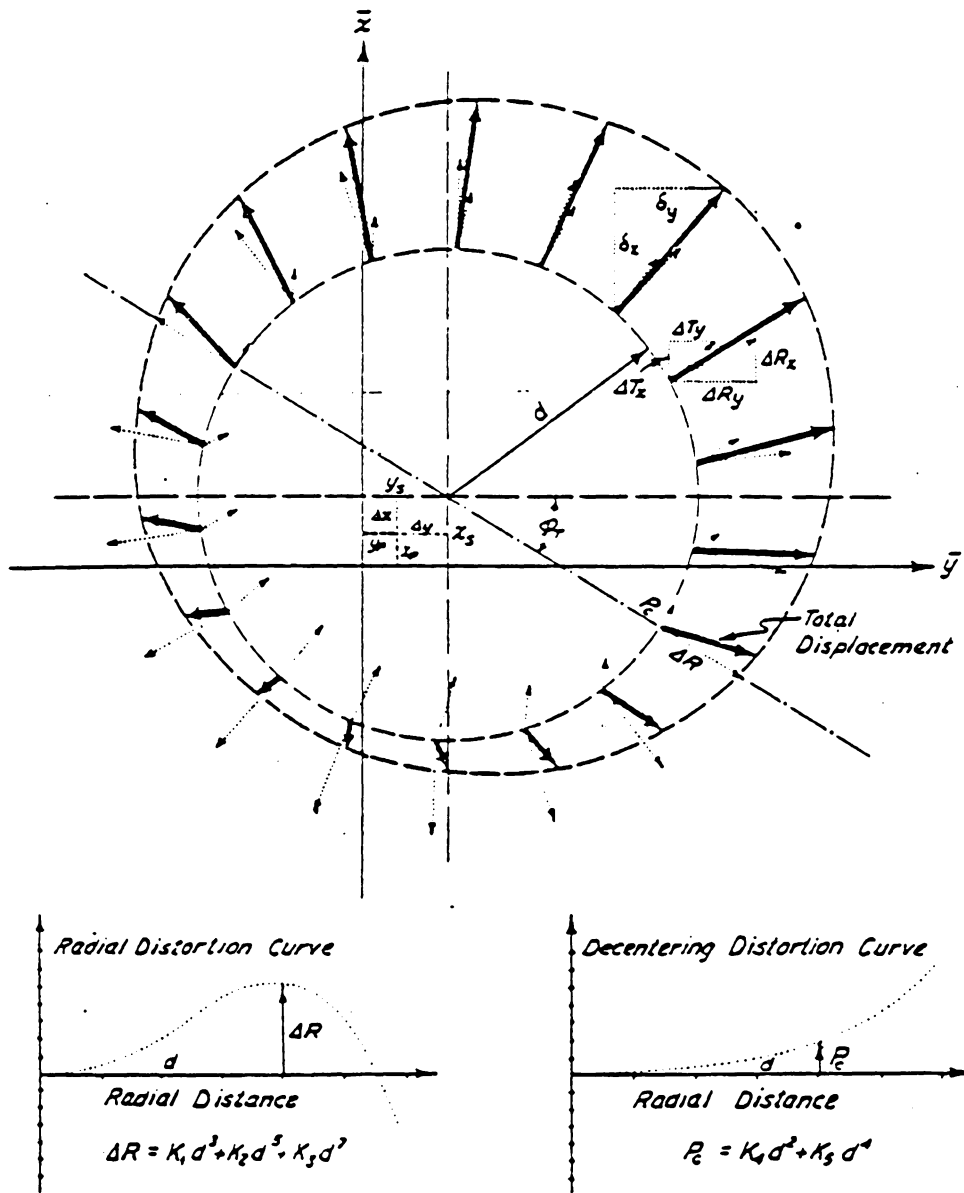


Figure 3.4 Combined Radial and Decentered Lens Distortion  
(Slama, 1972)

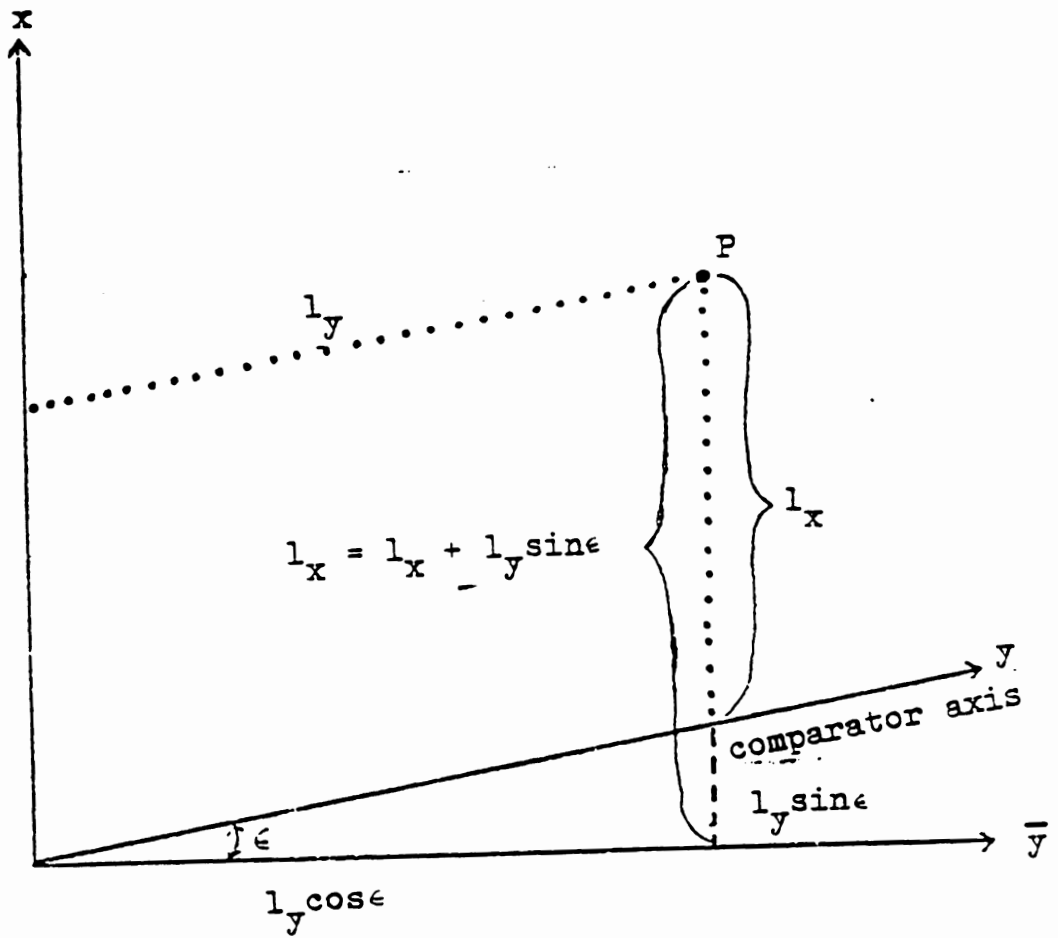


Figure 3.5 Nonperpendicularity of the Comparator Axis  
(Slama, 1972)

space(measured plate coordinates) are

$$\tilde{x}_i = \left(\frac{C_{x^m}}{q} + x_p\right)\left(1 + \frac{\Delta R}{d} + D_x\right) - x_s\left(\frac{\Delta R}{d} + D_x\right) - y_i \quad (3.16)$$

$$\tilde{y}_i = \left(\frac{C_{y^n}}{q} + y_p\right)\left(1 + \frac{\Delta R}{d} + D_y\right) - y_s\left(\frac{\Delta R}{d} + D_y\right) \quad (3.17)$$

### 3.1.4 Least Squares Observation Equations

The linearized observations equations are of the form

$$l_x + v_x = \tilde{x}_i^0 + \left(\frac{\partial x_i^0}{\partial \mu^0}\right) \Delta \mu^0 \quad (3.18)$$

$$l_y + v_y = \tilde{y}_i^0 + \left(\frac{\partial y_i^0}{\partial \mu^0}\right) \Delta \mu^0 \quad (3.19)$$

where

$l_x, l_y$  = are the measured plate observations

$v_x, v_y$  = are the unknown residuals

$x_i, y_i$  = are expressions (1) and (2) evaluated with the approximations for the unknown parameters from which estimates of the unknowns are given by

$$\hat{\mu} = \mu^0 + \Delta \mu^0$$

$\frac{\partial x_i^0}{\partial \mu^0}, \frac{\partial y_i^0}{\partial \mu^0}$  = are partial derivatives of  $\tilde{x}_i^0$  and  $\tilde{y}_i^0$  with respect to each of the unknown parameters.

The unknown parameters are:

$\alpha, \delta$	star image coordinates
$\alpha, \omega, \delta^i$	angle of nonperpendicularity
$x_p, y_p$	coordinates of the principal point
$C$	calibrated focal length
$x, y$	point of symmetry translation parameters
$K_1, K_2, K_3$	radial symmetric lens distortion model coefficients
$K_4, K_5$	decentered lens distortion model coefficients
$\theta_T$	orientation angle of axis of maximum tangential distortion.

### 3.1.5 Least Squares Adjustment

The coefficient matrix is of the form

$$B = \left[ B_0 \mid B_x \right] \quad (3.20)$$

where

$B_0$  = the partial derivatives of the expressions  $\hat{x}_i^0$  and  $\hat{y}_i^0$  with respect to  $\alpha$  and  $\delta$ ,

$B_x$  = the partial derivatives of the expressions  $\hat{x}_i^0$  and  $\hat{y}_i^0$  with respect to the remaining unknowns.

The set of resulting  $j$  normal equations has the following structure

$$\begin{bmatrix} N_1^* & 0 & 0 & \dots & 0 & \bar{N}_1 \\ 0 & N_2^* & 0 & \dots & 0 & \bar{N}_2 \\ 0 & 0 & N_3^* & \dots & 0 & \bar{N}_3 \\ \vdots & \vdots & \vdots & \ddots & \vdots & \vdots \\ \vdots & \vdots & \vdots & \ddots & \vdots & \vdots \\ \vdots & \vdots & \vdots & \ddots & \vdots & \vdots \\ 0 & 0 & 0 & \dots & N_j^* & \bar{N}_j \\ \hline \bar{N}_1^T & \bar{N}_2^T & \bar{N}_3^T & \dots & \bar{N}_j^T & \mathbf{N} \end{bmatrix} \begin{bmatrix} \Delta_1 \\ \Delta_2 \\ \vdots \\ \vdots \\ \vdots \\ \vdots \\ \Delta_j \\ \mathbf{T} \end{bmatrix} = \begin{bmatrix} t_1 \\ t_2 \\ t_3 \\ \vdots \\ \vdots \\ \vdots \\ t_j \\ \mathbf{T} \end{bmatrix} \quad (3.21)$$

Let  $n$  equal the number of observations of a star. Thus,

$$N_j^* = \left( \sum_{i=1}^n B_{x_i}^T W_i B_{x_i} \right)_j + W_{\alpha S} \quad , \quad (3.22)$$

$$\bar{N}_j = \left( \sum_{i=1}^n B_{x_i} W_i B_{o_i} \right)_j \quad , \quad (3.23)$$

$$t_j = \left( \sum_{i=1}^n B_{x_i} W_i t_i \right)_j \quad (3.24)$$



where

$$\Delta t_n = \begin{bmatrix} t_{x_n} - \hat{x}_n \\ t_{y_n} - \tilde{y}_n \end{bmatrix} .$$

The matrices for  $N$  and  $t$  represent summations, over all  $n$  observations of all  $j$  stars in the problem, of

$$\begin{aligned} N = & \left( \sum_{i=1}^n B_{o_i}^T W_i B_{o_i} \right)_1 + \left( \sum_{i=1}^n B_{o_i}^T W_i B_{o_i} \right)_2 + \\ & \dots + \left( \sum_{i=1}^n B_{o_i}^T W_i B_{o_i} \right)_j + W_o \end{aligned} \quad (3.25)$$

and

$$\begin{aligned} t = & \left( \sum_{i=1}^n B_{o_i}^T W_i t_i \right)_1 + \left( \sum_{i=1}^n B_{o_i}^T W_i t_i \right)_2 + \\ & \dots + \left( \sum_{i=1}^n B_{o_i}^T W_i t_i \right)_j + W_o t_o . \end{aligned} \quad (3.26)$$

For development of the coefficients, all weight matrices and  $t$  see Slama(1976).

The normal equations have the following structure,

$$\begin{bmatrix} \mathbf{N}^* & \bar{\mathbf{N}} \\ \bar{\mathbf{N}}^T & \mathbf{N} \end{bmatrix} \begin{bmatrix} \Delta_1 \\ \Delta_2 \end{bmatrix} = \begin{bmatrix} t \\ \mathbf{T} \end{bmatrix} \quad (3.27)$$

which leads to the reduced normal equation system,

$$(\mathbf{N} - \bar{\mathbf{N}}^T \mathbf{N}^{*-1} \bar{\mathbf{N}}) \Delta_2 = (\mathbf{T} - \bar{\mathbf{N}}^T \mathbf{N}^{*-1} t) \quad (3.28)$$

thus eliminating the unknown parameters associated with the star observations.

The solution is iterated until the change in the sums of squares of the residuals converge below a pre-specified tolerance. The data for each of the four photographs is processed independently through the Single Camera Orientation program. This results in four separate solutions for the same set of interior orientation and distortion parameters.

### 3.2 Multiplate Camera System Calibration Program

The results from the Single Camera Orientation program for each of the four plates are combined and readjusted in the Multi-plate Camera Stellar Calibration program. This

program uses as input the inverse of the reduced normal equations from each of the four solutions of the Single Camera Orientation program. The values for the unknown parameters from the four solutions are used as initial approximations. All of the data is combined in a grand simultaneous least squares adjustment to obtain, according to Fritz(1976), individual exterior orientations for each photograph and one set of interior orientation and lens distortion calibration parameters for the aperture-filter combination used.

### 3.3 Flow Diagram

The Flow Diagram concept was developed by Yourdon (1982). A Flow Diagram is a Network Representation of a system(automated, manual, or mixed). It declares the component pieces of the system, and the interfaces between them.

The Flow Diagram consists of the following four elements:

The Flow - a pipeline through which packets of known composition flow. The notation for it is a "named" vector which usually takes the name of the packet.

The Transformation Process - a transformation of incoming flow(s) into outgoing flow(s). Its notation is a circle or bubble containing a name and usually a number.

The Store - a time-delayed repository of information or material. It is represented by straight line

segment(s) with an associated name.

The Terminator - a person, system, or organization lying outside context of the study, which is a net source or receiver of flows that are part of the study. It is represented by a box enclosing the name of the terminator.

The first page of the Flow Diagram shows the Large Format Camera calibration process divided into six major parts or "bubbles". Each bubble contains a heading and an assigned number. For example, bubble #1 is titled "Grid Calibration". Since the Grid Calibration process needed further explanation it was divided into several more bubbles which are shown on the second page of the Flow Diagram. These bubbles refer back to bubble #1, and they are accordingly numbered 1.1, 1.2, 1.3, etc.. If one of these bubbles needs to be broken down further, say bubble #1.2, its divisions will be numbered 1.21, 1.22, 1.23, etc., and placed on another page. This process continues for as many divisions as needed for any particular bubble.

Any bubble which contains a letter as well as a number is keyed to Table 3.1. Table 3.1 contains a list of the computer programs used by the National Ocean Service for the Large Format Camera calibration. The programs are broken down into groups based on the computer on which they were run.

Table 3.1 Large Format Camera Computers and Programs

Univac 1100/43

- A - LOCAL SIDEREAL TIME
- B - MEAN
- C - MNWTMN
- D - PRELIMINARY CAMERA ORIENTATION
- E - SHEAR
- F - STAR PLOT

PDP-11

- G - EDIT
- H - MULTI-PLATE CAMERA STELLAR SYSTEM

UNIVAC/FR80

- K - PLOTS

CDC

- I - SINGLE CAMERA ORIENTATION
- J - STARID

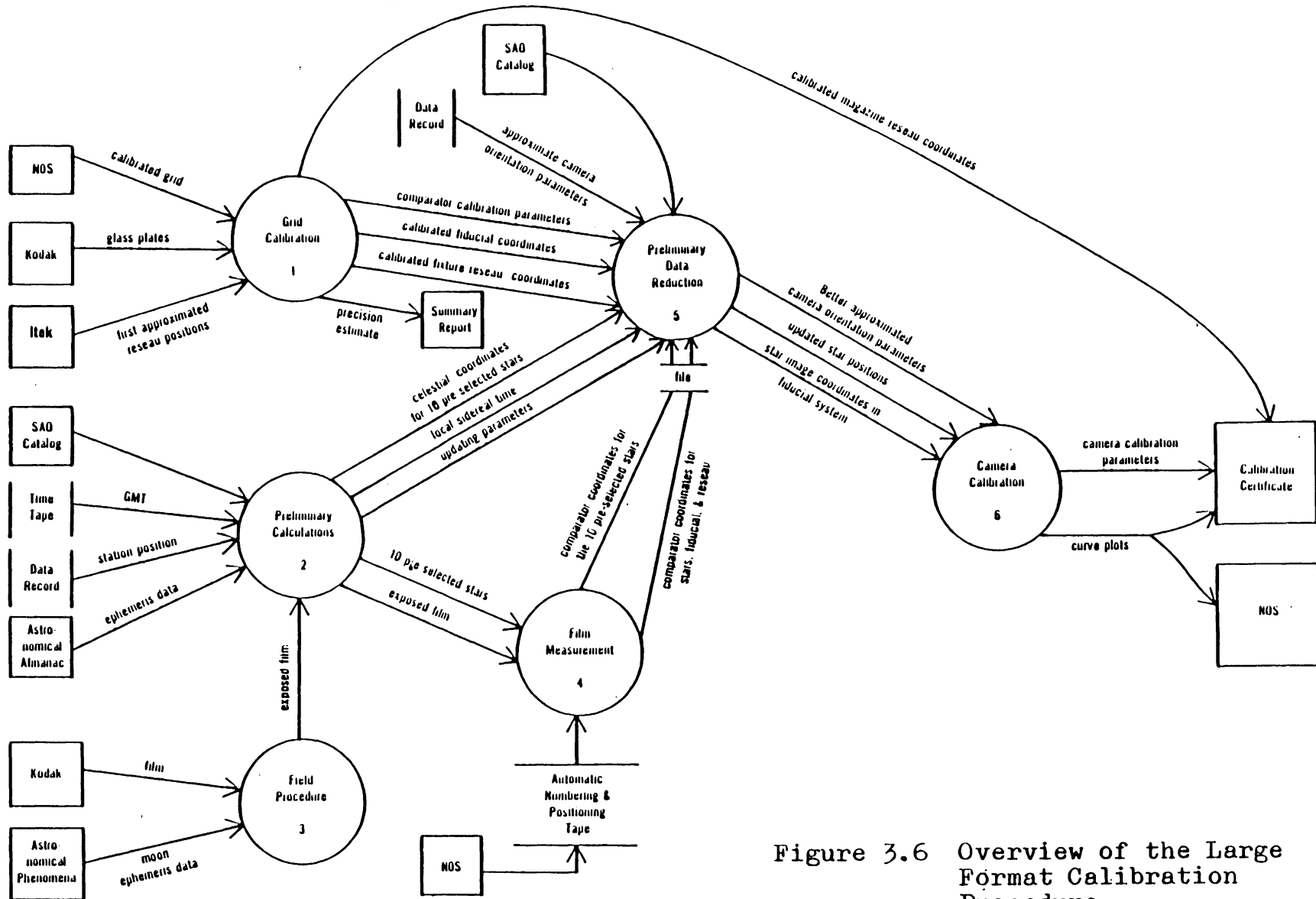


Figure 3.6 Overview of the Large Format Calibration Procedure

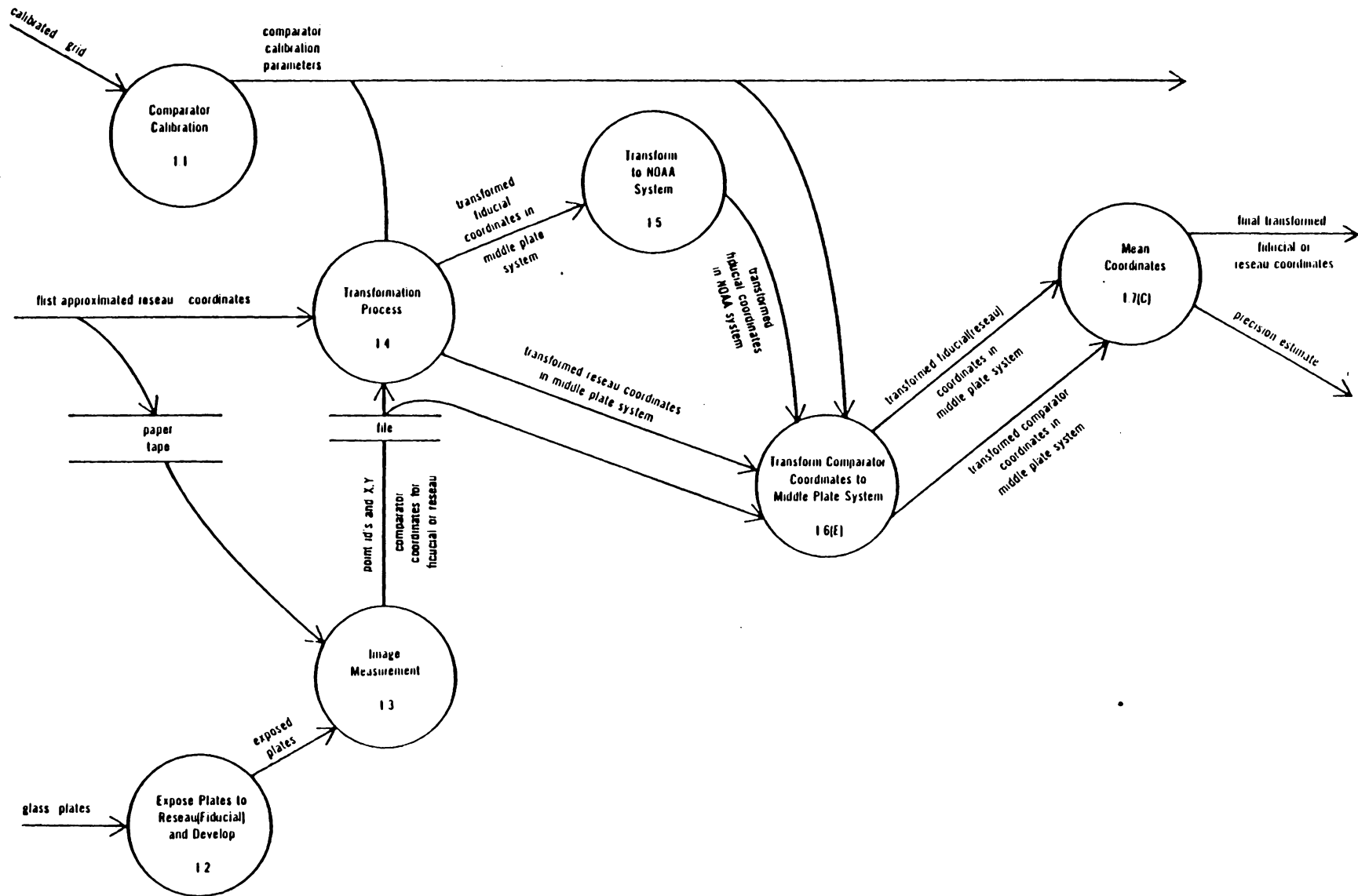


Figure 3.7 Grid Calibration Process

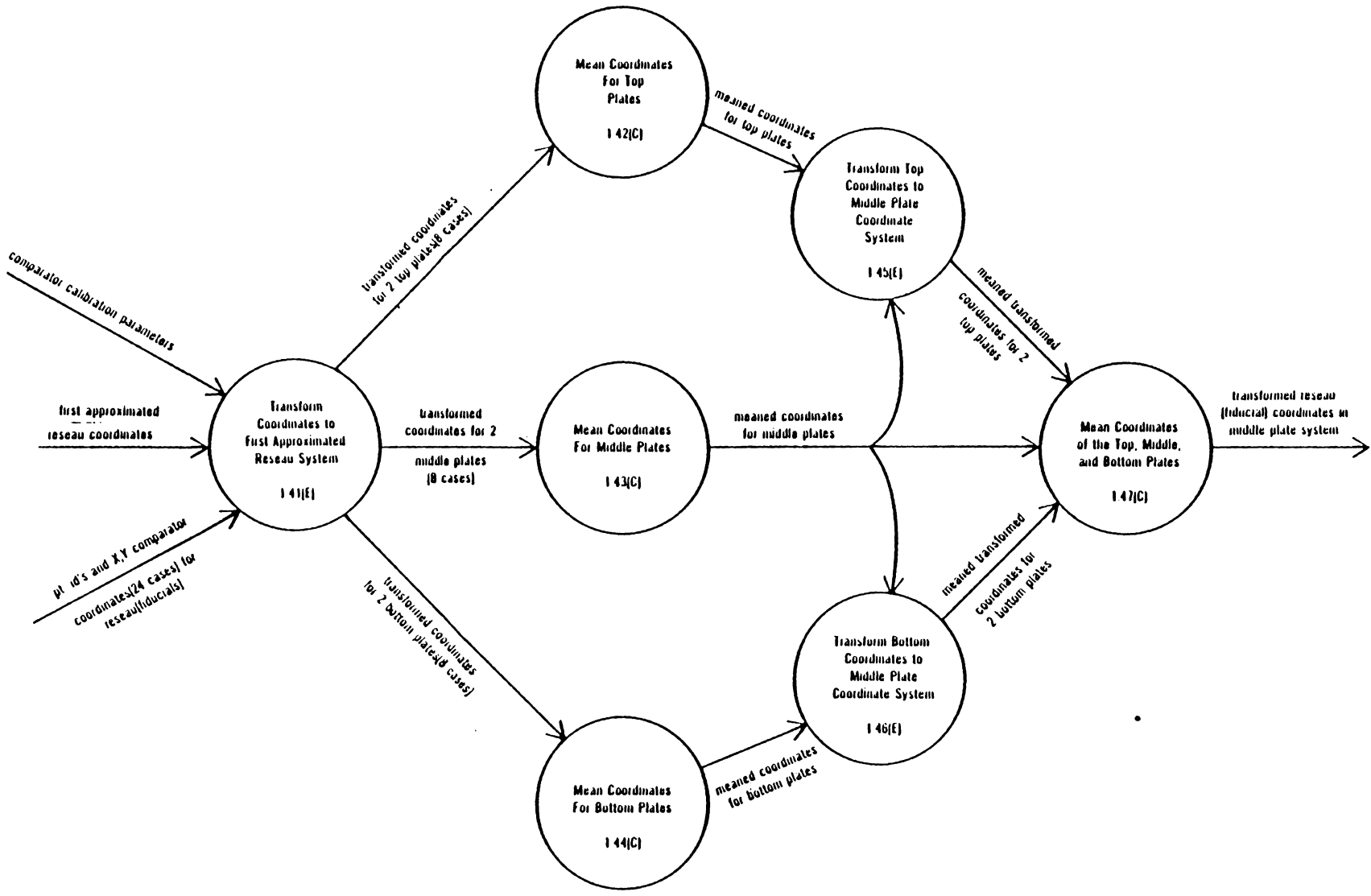


Figure 3.8 Grid Coordinate Transformation Process



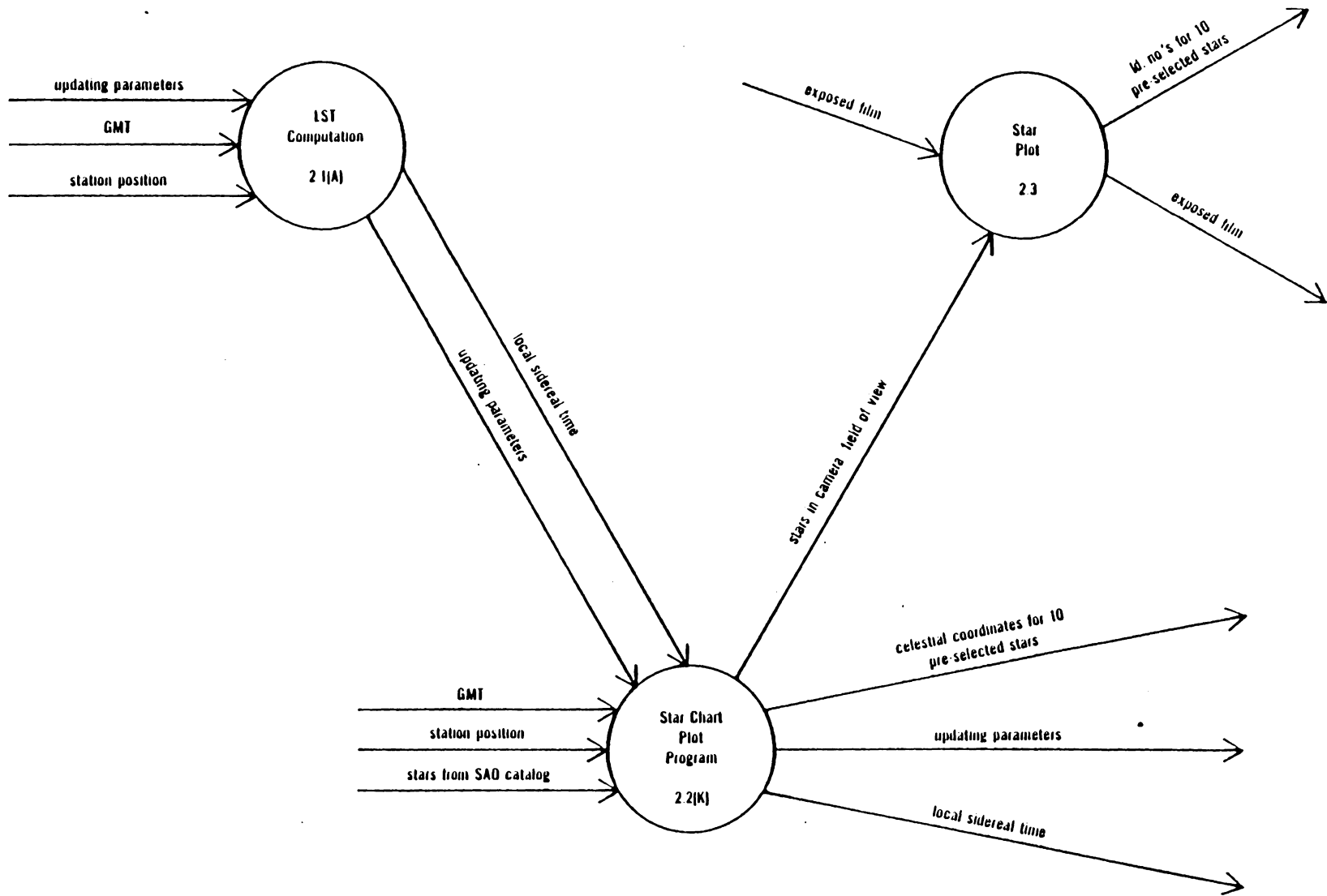


Figure 3.9 Preliminary Calculations

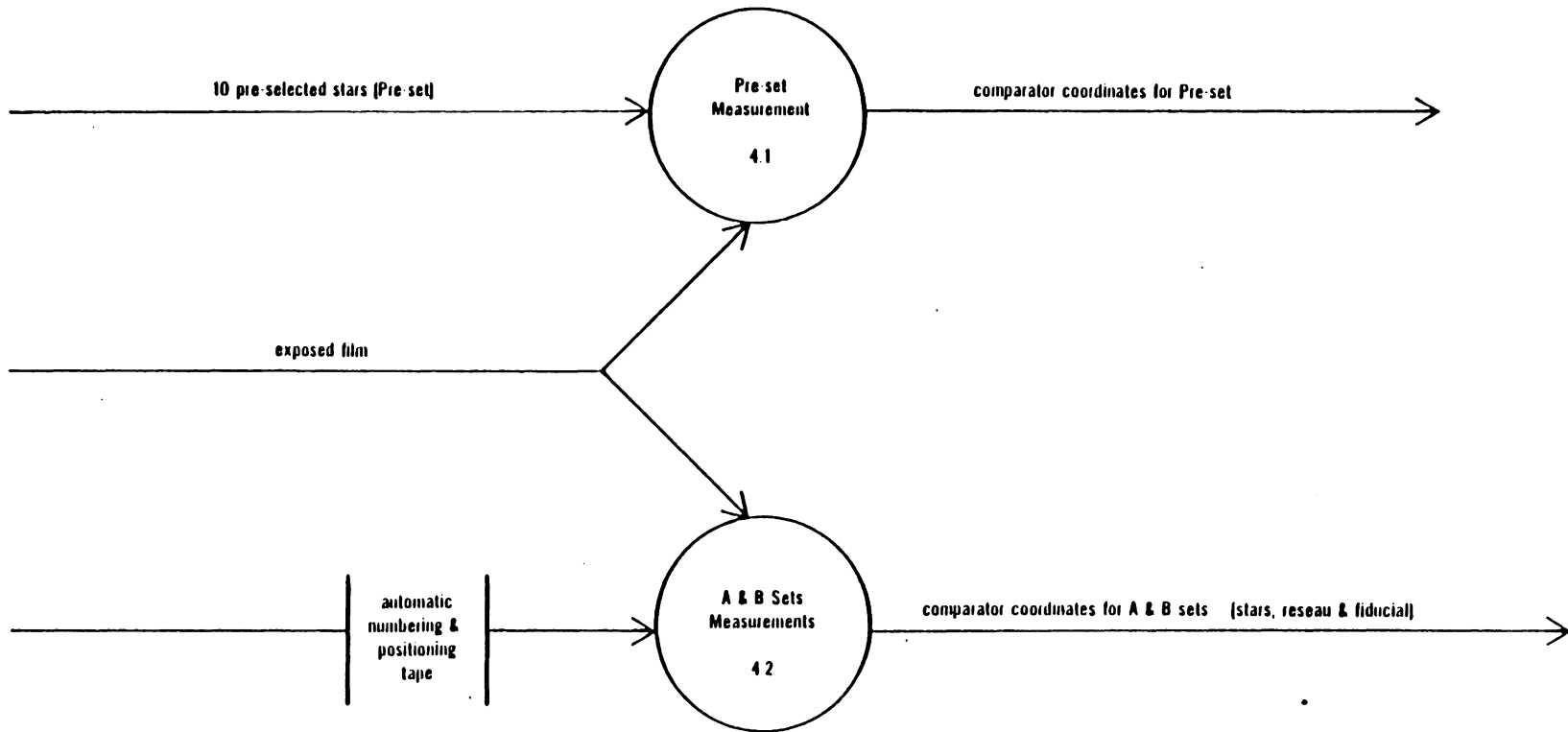


Figure 3.10 Film Measurement

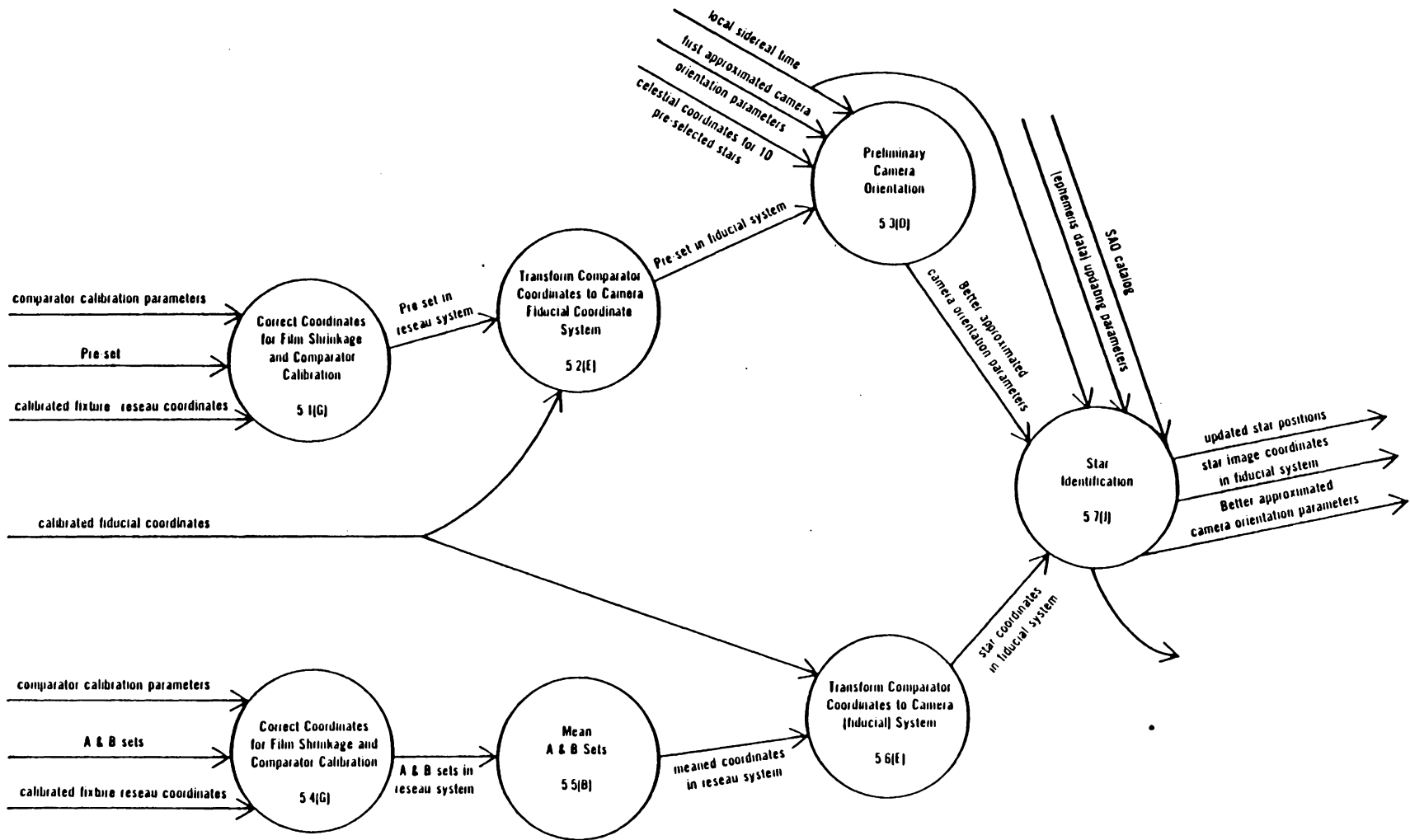


Figure 3.11 Preliminary Data Reduction

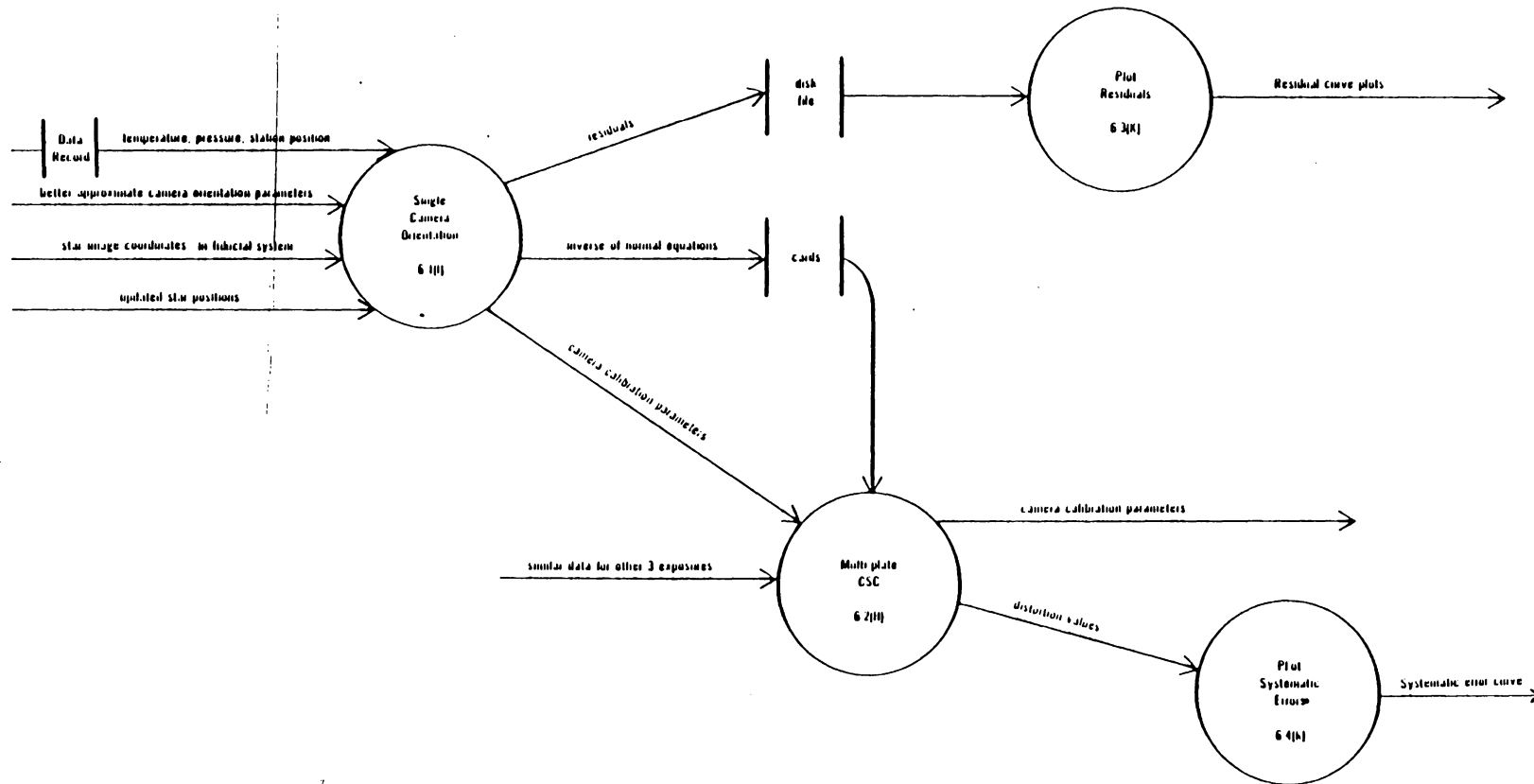


Figure 3.12 Camera Calibration

## 4. CALIBRATION RESULTS

The end product of the camera calibration procedure is the calibration certificate. It contains all of the pertinent data and information which is needed in any future photogrammetric computations relating to photographs exposed in the camera. This chapter will deal with some of the results and diagnostic plots which are included in the certificate of calibration for the Large Format Camera. The computed values for the calibration parameters as determined by the least squares reduction are given in the Appendix. Also included in the Appendix are the calibrated fiducial and magazine reseau coordinates.

### 4.1 Application Equations

This section describes the steps for applying the calibrated lens distortion parameters to measured image points. The following is a list of calibrated parameters which will be used in the subsequent equations.

$x_s, y_s$	point of symmetry coordinates
$K_1, K_2, K_3$	radial symmetric lens distortion model coefficients
$K_4, K_5$	decentering lens distortion model coefficients
$\phi_T$	orientation angle of axis of maximum tangential distortion

- 1) Correct measured coordinates for comparator errors (particular to the comparator used to measure the

images).

- 2) Use the magazine reseau coordinates to correct for film deformation.
- 3) Rotate and translate refined coordinates into the fiducial coordinate system. This can be achieved by using a two-dimensional linear conformal transformation which allows for a rotation, a uniform scale change and two translations.

Coordinates must be in meters for the following steps.

- 4) Compute radial distance( $d$ ) for point  $(x_m, y_m)$  from point of symmetry  $(x_s, y_s)$ .

$$dx = x_m - x_s$$

$$dy = y_m - y_s$$

$$d^2 = dx^2 + dy^2$$

- 5) Compute the corrections for lens distortions.

$$\text{Radial: } \frac{\Delta R}{d} = K_1 d^2 + K_2 d^4 + K_3 d^6$$

$$\text{Decentered: } \Delta T = K_4 d^2 + K_5 d^4$$

- 6) Compute the corrected coordinates( $x^*, y^*$ ) for the measured image point.

$$x^* = x_m - \frac{\Delta R}{d}(dx) - \Delta T \left[ \frac{2dx dy}{d^2} \sin \theta_T + \left( \frac{2dx^2}{d^2} + 1 \right) \cos \theta_T \right]$$

$$y^* = y_m - \frac{\Delta R}{d}(dy) - \Delta T \left[ \frac{2dx dy}{d^2} \cos \theta_T + \left( \frac{2dy^2}{d^2} + 1 \right) \sin \theta_T \right]$$

To be absolutely correct, distortion should be computed by successive approximation as described by Slama(1972).

#### 4.2 Distortion Plots

Figure 4.1 shows the Radial Symmetric Distortion curve which represents the linear distortion characteristic of the Large Format Camera lens. It was plotted with image radial distances from the lens axis as abscissas and image radial displacements as ordinates. The curve is based on the calibrated focal length. In Figure 4.2, a transformed calibrated focal length was computed such that the area under each lobe of the radial symmetric distortion curve is equivalent. The lens decentering distortion curve is shown in Figure 4.3. It depicts the distortion profile for distances from the point of symmetry along the axis of maximum tangential distortion( $\theta_T$ ). The dotted line in each of these three figures represent a one-sigma envelope of

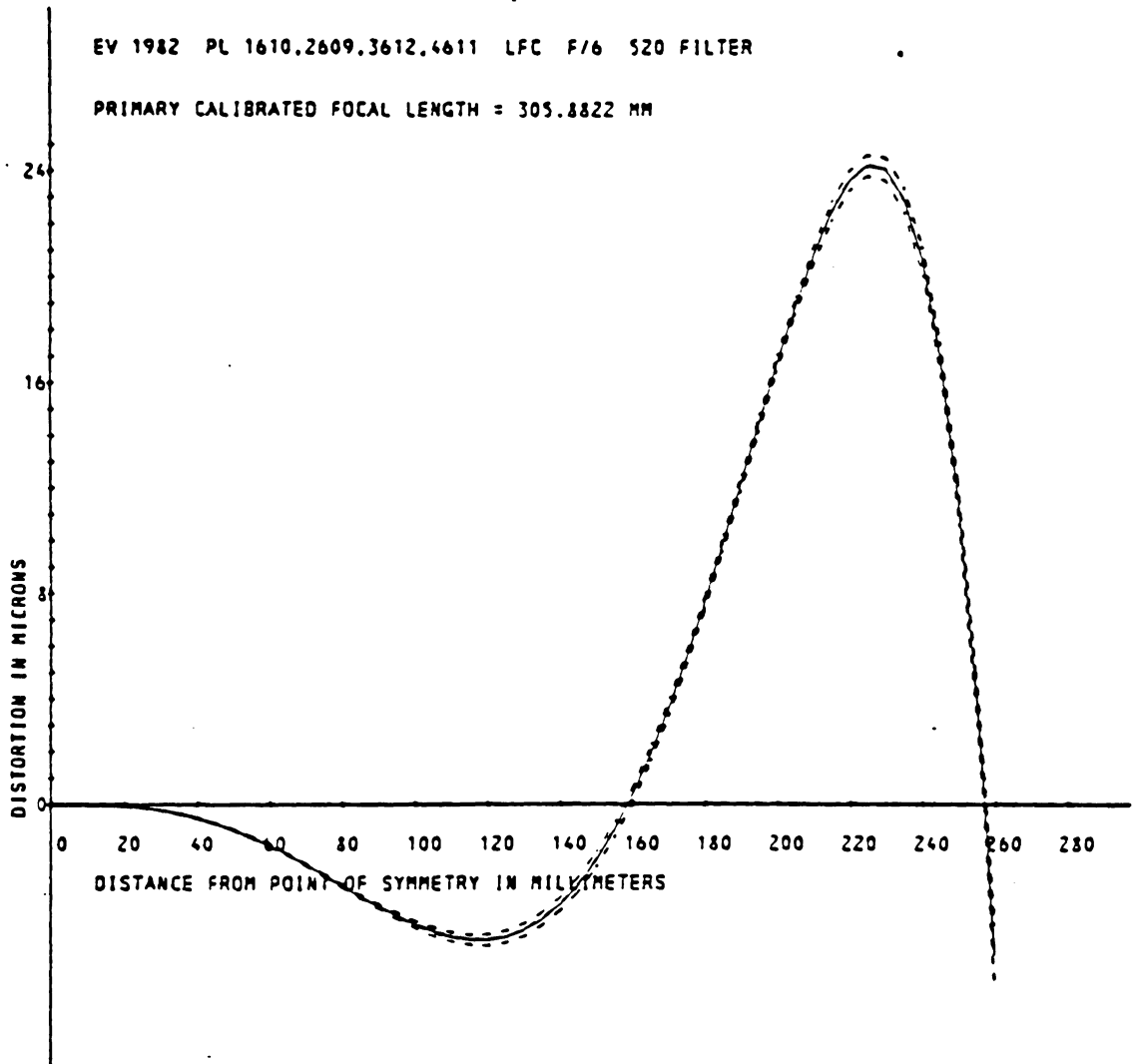
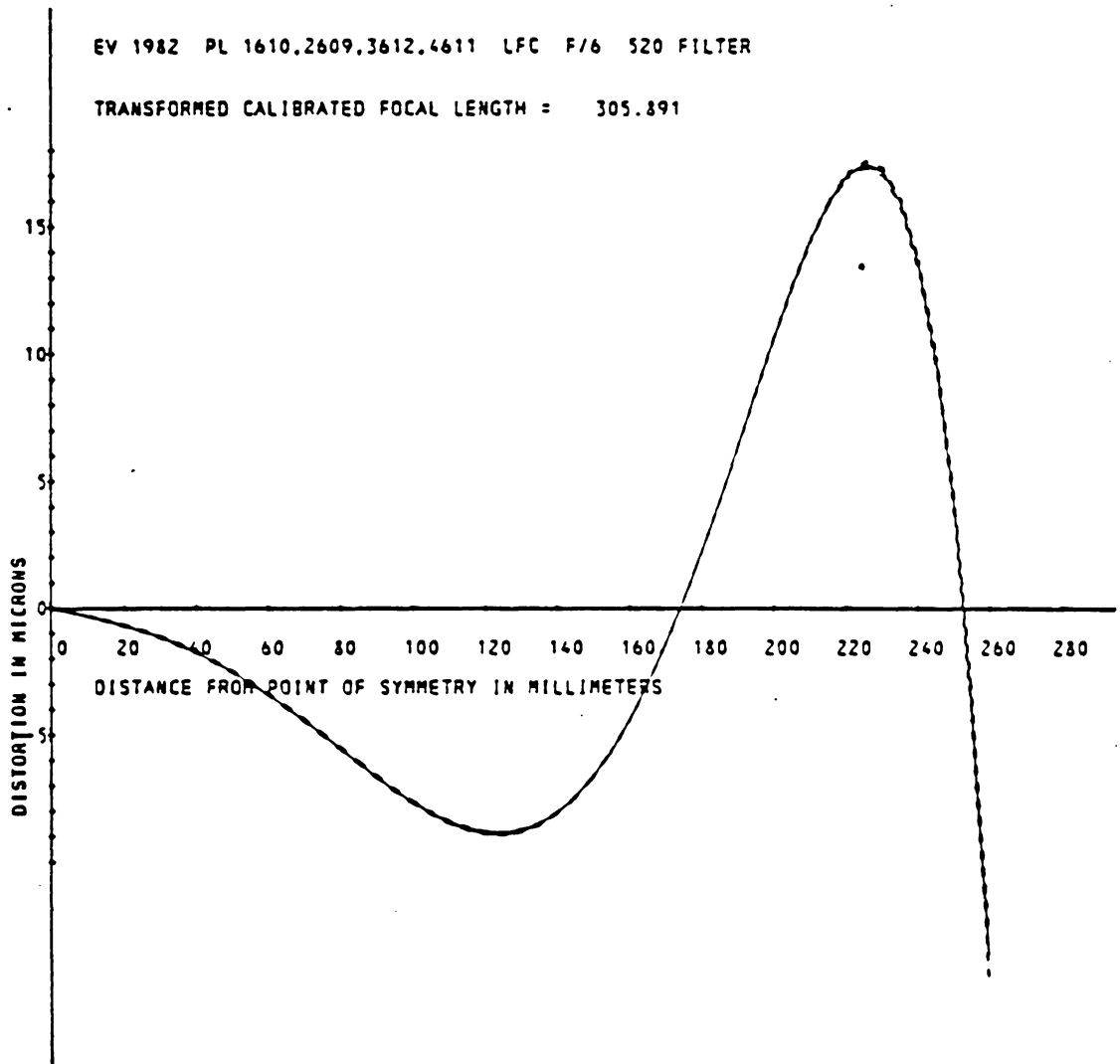


Figure 4.1 Radial Symmetric Distortion Curve  
(Report of Calibration by Stellar Method, 1983)





transformed to balance the area under the curve

Figure 4.2 Transformed Radial Symmetric Distortion Curve  
(Report of Calibration by Stellar Method, 1983)

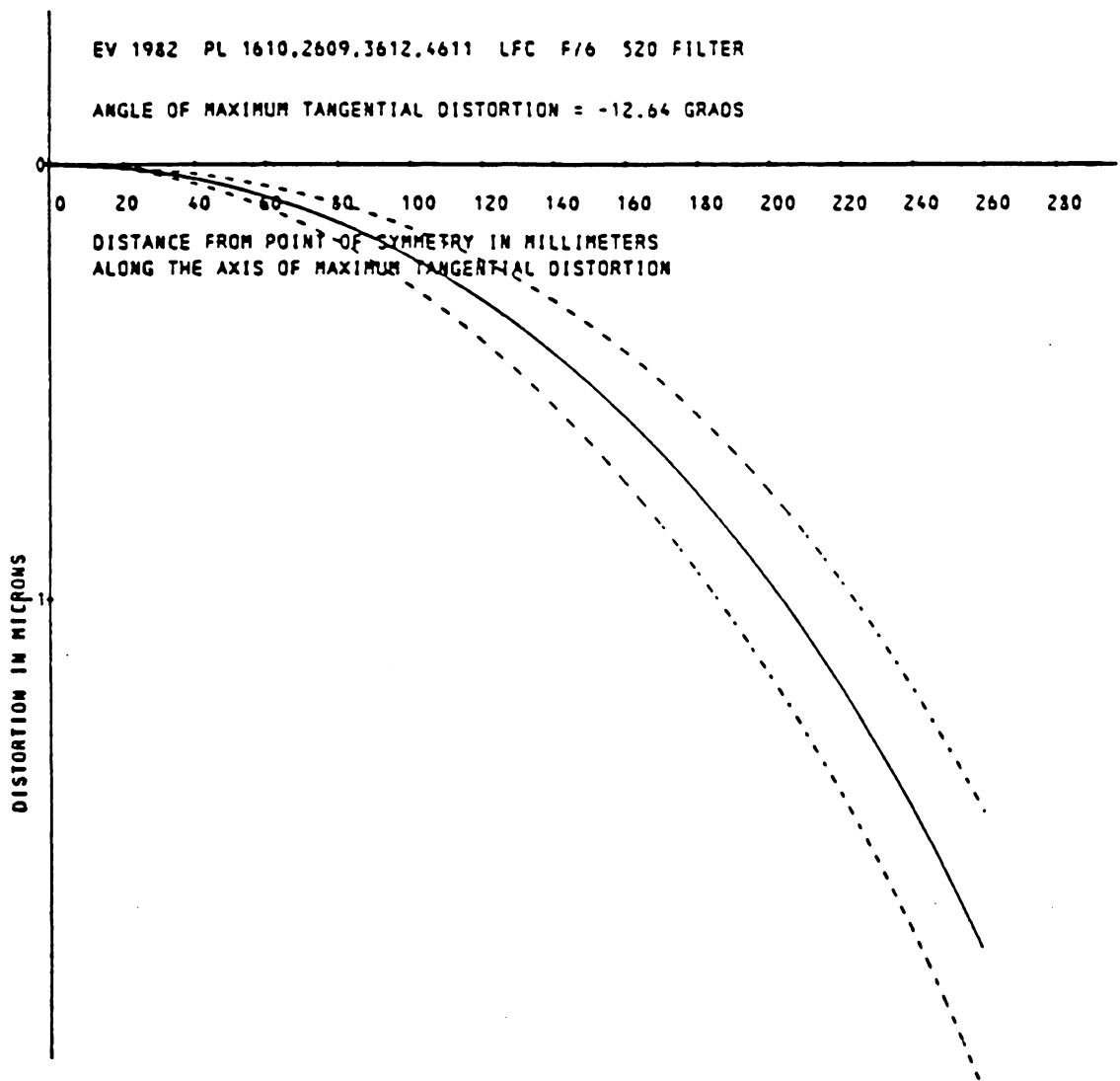


Figure 4.3 Lens Decentering Distortion Curve  
(Report of Calibration by Stellar Method, 1983)

curve accuracy.

### 4.3 Systematic Distortion Plots

Figures 4.4, 4.5, and 4.6 show distortion in microns at points over the format of the Large Format Camera. Figures 4.4 and 4.5 are plots of the radial symmetric lens distortion and lens decentration distortion respectively. A plot of the total math model of systematic distortion is shown in Figure 4.6.

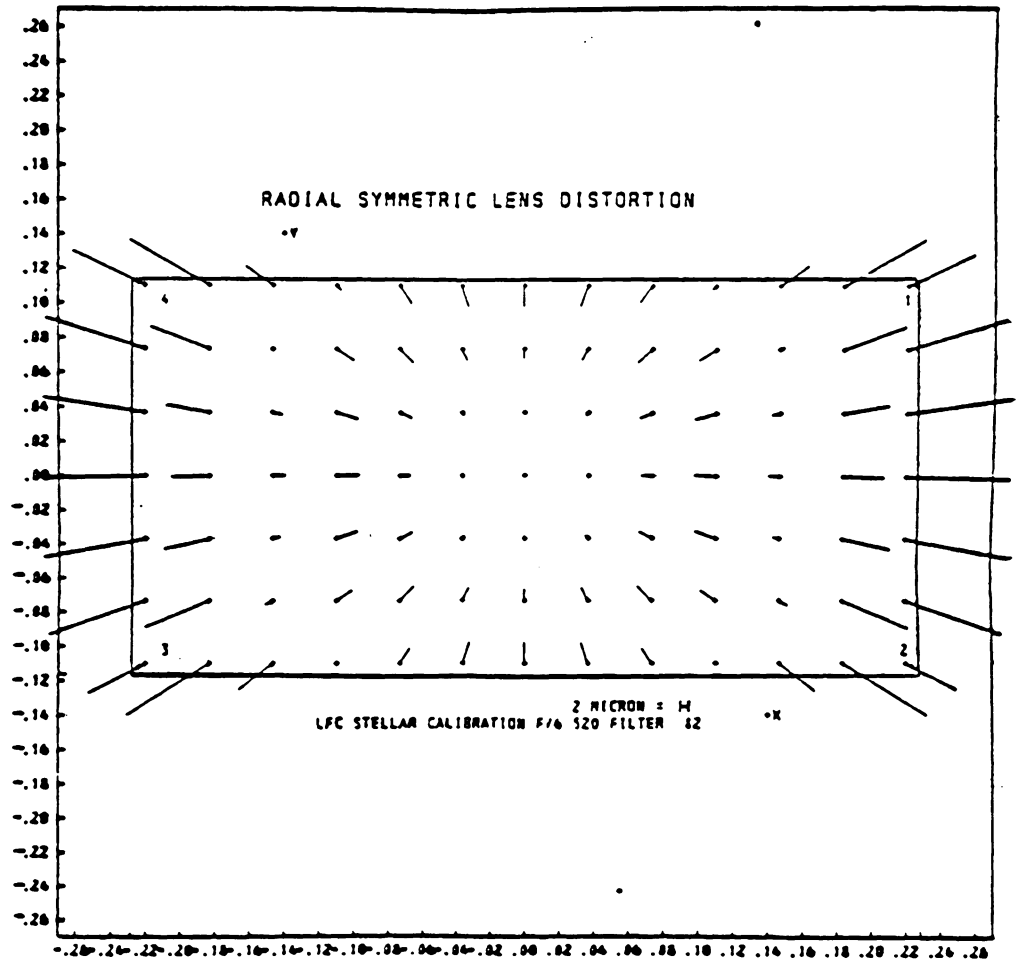


Figure 4.4 Radial Symmetric Lens Distortion  
 (Report of Calibration by Stellar Method, 1983)

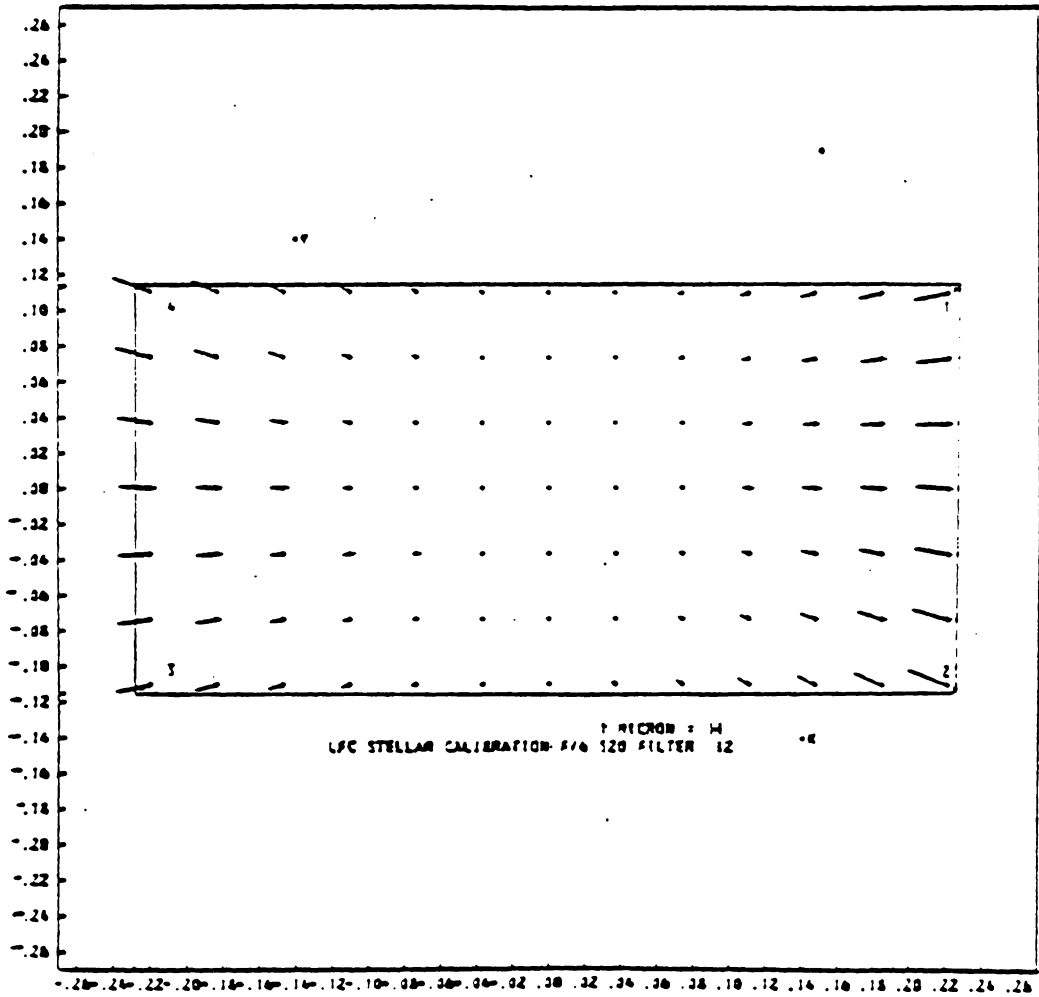


Figure 4.5 Lens Decentration Distortion  
 (Report of Calibration by Stellar Method, 1983)

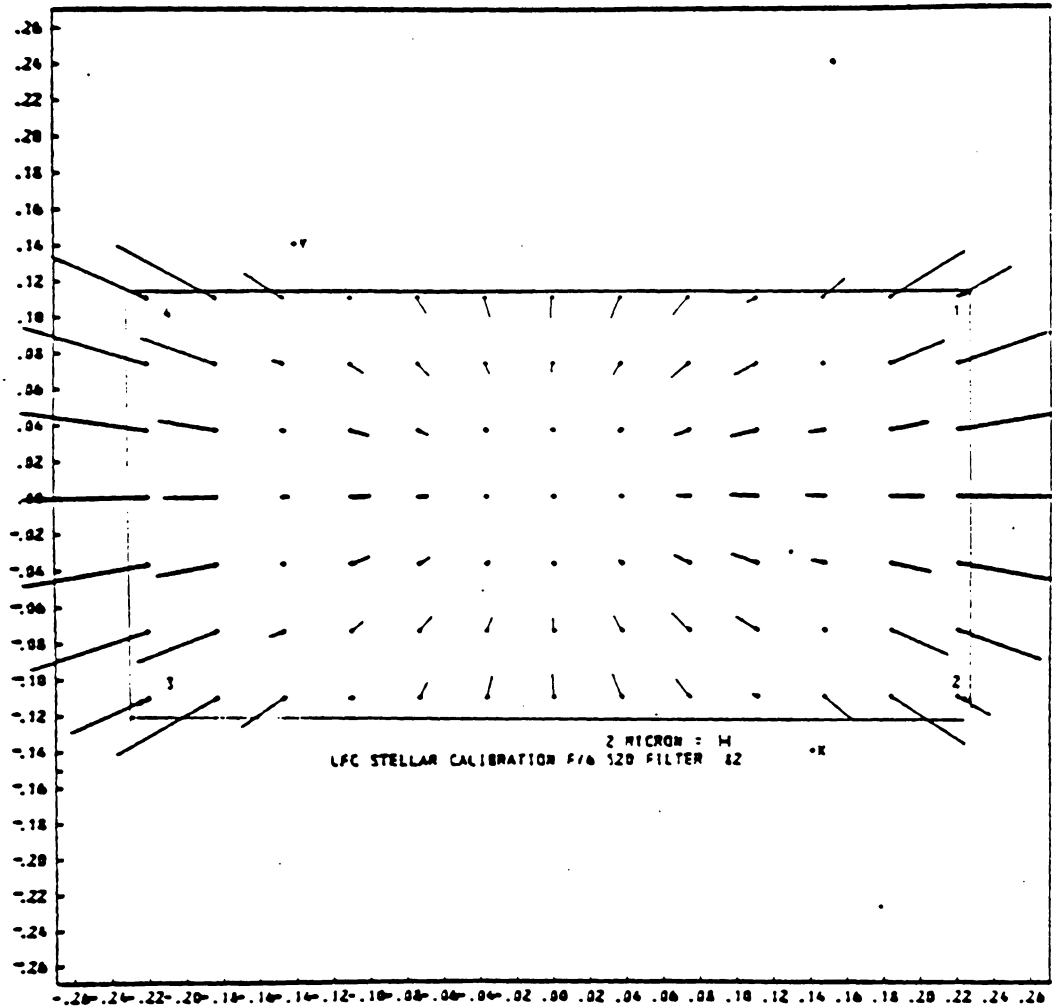


Figure 4.6 Total Math Model of Systematic Distortion  
(Report of Calibration by Stellar Method, 1983)

## 5. CONCLUSIONS

The primary design objective for the Large Format Camera was to maximize all system performance characteristics while maintaining a high level of reliability compatible with rocket launch conditions and the on-orbit environment. It was also designed to meet the rigors of space applications.

Other requirements included superior spatial resolution in the visible and near infrared spectra, and minimum geometric distortion for precision cartographic applications. It was also designed to provide wide-area stereoscopic imagery for mineral and fossil fuel exploration.

Table 5.1 summarizes a few of the requirements for the Large Format Camera parameters and their corresponding National Ocean Service stellar calibration results.

As can be seen by these results, the Large Format Camera has met these design specifications.

Table 5.1 Design Requirements vs. Stellar Calibration Results

	<u>Design Requirement</u>	<u>Stellar Calibration</u>
focal length	$304.8 \pm 5$ mm	305.8822mm
radial symmetric distortion	$D_{\max} \pm .025$ mm	.024 mm -.005 mm
decentered distortion	no requirement	-.0017 mm



## 6. SUMMARY

Initially, the Large Format Camera will be carried into Earth orbit by the Space Shuttle. However, future considerations include mounting the camera in a free-flying spacecraft. The spacecraft can be placed in near-polar orbit, remaining operational for many months. The film would be recovered and returned to Earth by the Shuttle.

The following list contains some of the applications for the imagery obtained by the Large Format Camera.

1. Cartographic
2. Environmental
3. Geological

There are many reasons why the Large Format Camera images will be advantageous to use over conventional small scale aerial photography.

For cartographic applications, the large area covered by a single space image results in significant savings of time and money in the process of compiling and updating regional maps. Large Format Camera images can be used directly for topographic compilation and update using existing techniques and equipment. The images will also supply the need for, on a worldwide basis, map coverage for economic planning and development.

Geological applications include mineral and fossil fuel exploration. The Large Format Camera's vertical,

maplike format will be easy to use for interpretation and mapping with existing techniques and equipment. The benefits of the Large Format Camera photography for geological exploration include reduced time and cost for exploitation of new finds.

Many federal agencies will utilize the photography from the Large Format Camera. These include the U. S. Geological Survey, U. S. Forest Service, and Environmental Protection Agency as well as the National Ocean Service.

Some of the intended applications for the photography by these agencies are

1. Compilation and revision of topographic maps and orthophotos,
2. Preparation of orthophoto and planimetric base maps for forest resource management,
3. Revision of shorelines, ports and harbors on nautical charts.

Therefore, the photography obtained by the Large Format Camera will be used to benefit many people.

## BIBLIOGRAPHY

- Anderson, James M., and Clement Lee, Analytical In-Flight Calibration, Photogrammetric Engineering, v. 41, n. 11, pp. 1337-1348, 1975.
- Bush, Anna Mary, The Reduction of Photographic Plate Measurements for Satellite Triangulation, NOAA Technical Report NOS 60, 1973.
- Doyle, Frederick J., A Large Format Camera for Shuttle, Photogrammetric Engineering and Remote Sensing, Vol. 15, No. 1, pp. 73-78, 1979.
- Fritz, Lawrence W., Complete Comparator Calibration, NOAA Technical Report NOS 57, 1973.
- \_\_\_\_\_, Grid Calibration by Coordinate Transfer, NOAA Technical Report NOS 53, 1972.
- \_\_\_\_\_, and Chester C. Slama, Multi-plate, Multi-exposure Stellar Calibration, A Presented Paper for the XIII ISP Congress, Helsinki, Finland, 1976.
- \_\_\_\_\_, and Hellmut H. Schmid, Stellar Calibration of the Orbicon Lens, Photogrammetric Engineering, v. 40, n. 2, pp. 101-115, 1974.
- Golder, William (Photogrammetric Research Section, National Ocean Service, NOAA, Rockville, Md.), personal communication, 1983.
- Livingston, Robert G., Aerial Cameras, Manual of Photogrammetry, 4th edition, Chapter IV, p. 187, ASP, Falls Church, Va., 1980.
- Mikhail, Edward M., and Francis H. Moffitt, Photogrammetry,

Harper and Row, New York, 1980.

Mollberg, Vernard H., Minutes of the Orbiter Camera Payload System(OCPS) Customer Acceptance Readiness Review(CARR), Experiment Systems Division, Lyndon B. Johnson Space Center, Houston, Texas, 1980.

\_\_\_\_\_, Performance Characteristics for the Orbiter Camera Payload System's Large Format Camera(LFC), Standard paper for initial presentation to the Technical Symposium East '81 of the Society of Photo-Optical Instrumentation Engineers, 1979.

Perry, Les(Photogrammetric Research Section, National Ocean Service, NOAA, Rockville, Md.), personal communication, 1983.

Report of Calibration by Stellar Method, Photogrammetry Branch, National Ocean Service, NOAA, 1983.

Sewell, Eldon D., Aerial Cameras, Manual of Photogrammetry, 3rd edition, Chapter IV, p. 133, ASP, Falls Church, Va., 1966.

Slama, Chester C., A Mathematical Model for the Simulation of a Photogrammetric Camera Using Stellar Control, NOAA Technical Report NOS 55, 1972.

Space Shuttle Orbiter Camera Payload System Technical Proposal, Itek, v. 1, 1977.

Structured Design Workshop for Real Time Systems, Edition 1.1, Yourdon, Inc., 1982.

Wong, K. W., Basic Mathematics of Photogrammetry, Manual of Photogrammetry, 4th edition, Chapter II, p. 37, ASP, Falls Church, Va., 1980.

## APPENDIX

This Appendix contains data and diagrams which are not included in Chapter 4.

Figure A.1 shows the first page of the Camera Calibration certificate. It contains information about the Large Format Camera such as its serial number, nominal focal length, and the aperture and filter type used in the calibration. It also gives a brief description of the stellar calibration.

The fiducial and magazine reseau numbering systems are shown in Figure A.2 along with the definitions of the calibrated parameters in Figure A.3. The calibrated fiducial coordinates are given in Figure A.4. The calibrated magazine reseau coordinate system is shown in Table A.1.

Tables A.2 and A.3 are output from the Multi-plate Camera Stellar Calibration program. It is a listing of the camera calibration parameter values and the variance-covariance matrix associated with the parameters. The coordinates for the distortion curve plots included in Chapter 4 are given in Table A.4. These coordinates are also output from the Multi-plate Camera Stellar Calibration program.

As explained in Chapter 2, one stellar exposure was taken in each of the four 90 degree positions about the

Calibration No. 654-182

**UNITED STATES DEPARTMENT OF COMMERCE**  
**National Oceanic and Atmospheric Administration**  
 NATIONAL OCEAN SERVICE

## REPORT OF CALIBRATION BY STELLAR METHOD

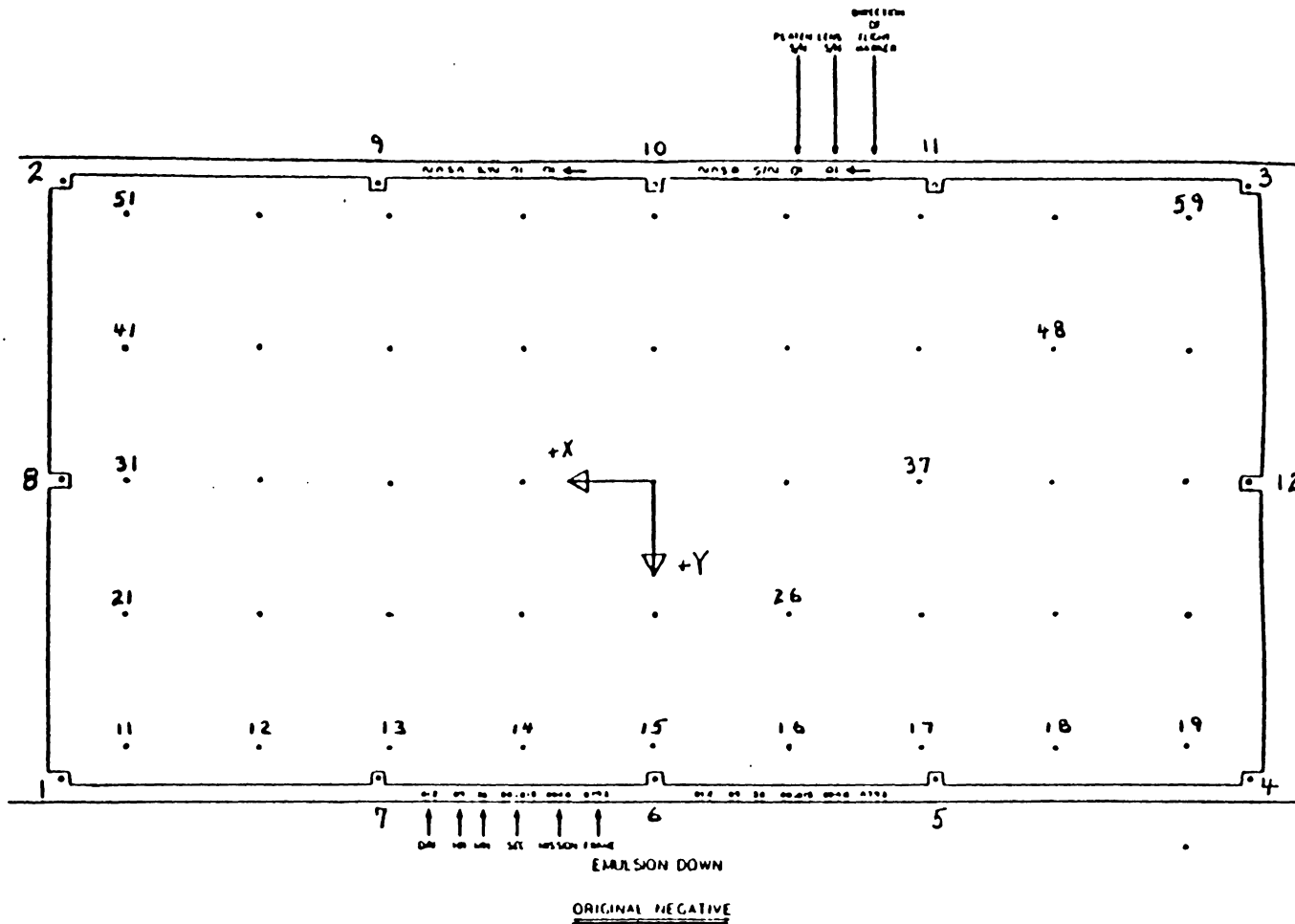
Prepared by

Photogrammetry Branch  
 Charting and Geodetic Services

Camera Type ITEK-NASA Large Format Camera  
 Effective Date of Calibration July 1982  
 Camera Serial No. 01  
 Lens and Cone Serial No. Metritek 01  
 Nominal Focal Length 306 mm  
 Aperture f/6  
 Filter 520 mu (intra lens)

**STELLAR CALIBRATION:** The NOS calibration by the stellar method is a high precision procedure that employs a series of accurately-timed exposures of a stellar field to determine the internal geometry of frame cameras and lens cones. That is, comparator-measured photo coordinates of star images are processed in a computer program, along with the directional coordinates of the stars, to define the mathematical orientation of the camera in inertial space. The computer program is based on a geometrical simulation of the camera central perspective augmented with all known physical perturbations present during the exposures or associated with the subsequent measuring process. The procedure employed produces the most comprehensive determination of camera constants available to the photogrammetric user.

Figure A.1 Large Format Camera Certificate of Calibration  
 (Report of Calibration by Stellar Method, 1983)



The fiducial coordinates and the magazine reseau coordinates are given in two independent coordinate systems.

Figure A.2 Fiducial and Magazine Reseau Numbering Systems  
 (Report of Calibration by Stellar Method, 1983)

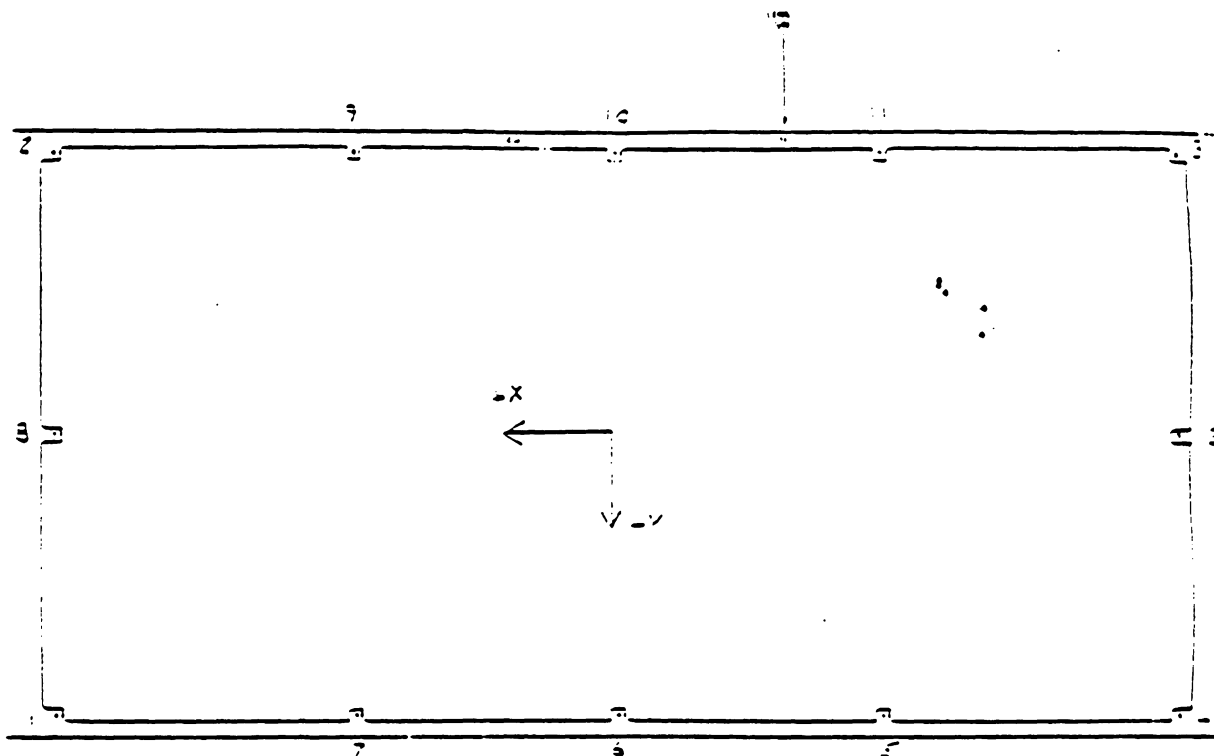
DEFINITION OF PARAMETERS: The 11 camera calibration parameters of the mathematical model are defined and symbolized as follows:

$C$	Primary calibrated focal length
$x_p, y_p$	Principal point coordinates
$x_s, y_s$	Point of symmetry coordinates
$K_1, K_2, K_3$	Radial symmetric lens distortion model coefficients
$K_4, K_5$	Decentering lens distortion model coefficients
$\Phi_T$	Orientation angle of axis of maximum tangential distortion

Figure A.3 Large Format Camera Calibration Parameters

(Report of Calibration by Stellar Method, 1983)





EMERSON COOR

ORIGINAL READING

Point No.	X	Y
1	223985.19	111984.57
2	223971.49	-111975.04
3	-223965.74	-111974.74
4	-223973.33	111976.06
5	-111967.32	111984.27
6	15.93	111992.24
7	111996.76	111996.30
8	223988.33	10.44
9	111978.24	-111963.13
10	3.16	-111963.49
11	-111965.42	-111972.37
12	-224048.36	4.34
	SIGMA X .7439	SIGMA Y .7267

The fiducial coordinates and the magazine reseau coordinates are given in two independent coordinate systems.

glass plates exposed and measured at 72°F

Figure A.4 Large Format Camera Calibration Fiducial Coordinates from a multi-plate(6) determination (Coordinates are given in micrometers)  
(Report of Calibration by Stellar Method, 1983)

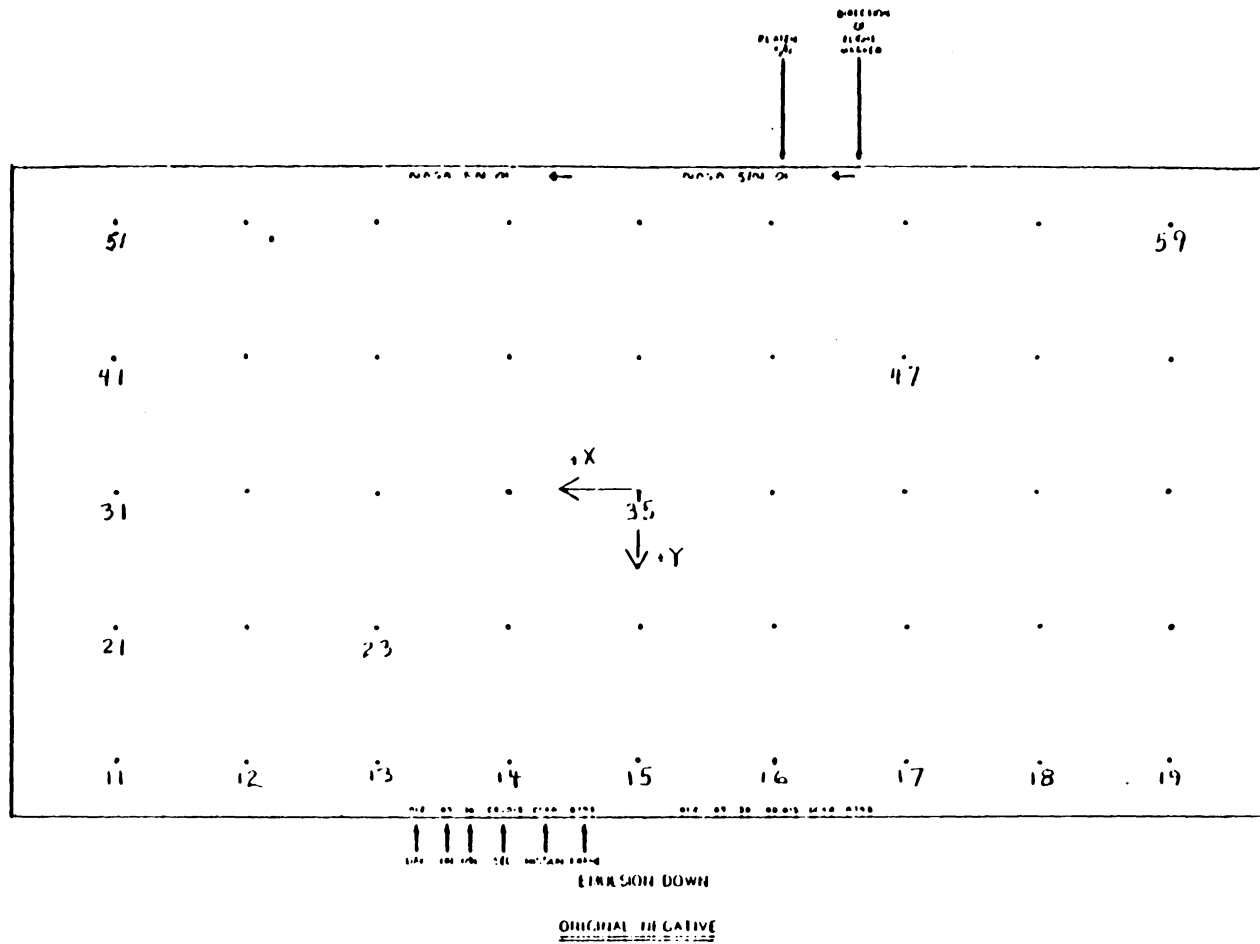


Figure A.5 Large Format Camera Magazine Reseau Coordinate System  
 (Report of Calibration by Stellar Method, 1983)

Table A.1 Large Format Camera Magazine Reseau Coordinates  
from a multi-plate(6) determination(Coordinates  
are given in micrometers)

(Report of Calibration by Stellar Method, 1983)

POINT NO	X	Y
11	199984.99	100011.29
12	149974.57	100006.63
13	99983.11	99998.61
14	49979.30	99999.53
15	-17.10	100008.43
16	-50010.74	100018.21
17	-100009.78	100004.81
18	-149997.16	99998.23
19	-200017.88	99977.58
21	199978.15	50020.77
22	149982.39	50017.71
23	99978.63	50010.50
24	49982.33	50022.43
25	23.49	50026.83
26	-50002.53	50012.39
27	-99992.49	50012.30
28	-149979.77	50018.61
29	-200008.38	49999.81
31	199984.14	29.84
32	149983.17	31.22
33	99977.26	28.69
34	49989.40	21.56
35	2.16	-1.62
36	-49974.25	26.03
37	-99997.25	2.28
38	-149995.19	22.84
39	-199989.76	6.16
41	199973.18	-49969.28
42	149974.53	-49960.04
43	99992.90	-49980.91
44	49993.94	-49993.15
45	7.85	-49997.31
46	-49989.86	-49975.60
47	-99984.00	-49992.36
48	-149990.13	-49994.31
49	-199974.69	-49984.01
51	200003.42	-99961.44
52	149997.19	-99961.80
53	99971.93	-99970.32
54	50007.62	-99975.67
55	11.10	-99962.62
56	-49975.95	-99983.96
57	-99983.17	-99974.47
58	-149990.23	-99983.51
	SIGMA X	SIGMA Y
	.9539	.8687

Measurements of point 59 on three glass plates indicated an "apparent"  
movement between exposures. DO NOT USE POINT 59 FOR FILM

DEFORMATION CORRECTION.

59	-200005.54	-99988.95
----	------------	-----------

Table A.2 Large Format Camera Calibration Parameters and Their Standard Errors from a Multi-exposure(4) determination (Report of Calibration by Stellar Method, 1983)

CALIBRATED FOCAL LENGTH	STANDARD ERROR
C = .3058822+000 M.	.5258821-006
C = 305.882 mm	

PRINCIPAL POINT	
COORDINATES	STANDARD ERROR
XP = .2151382-004 M.	.1225879-005
YP = .2414227-004 M.	.6286635-006
XP = 0.022 mm	
YP = 0.024 mm	

POINT OF SYMMETRY	
COORDINATES	STANDARD ERROR
XS = -.9156031-003 M.	.3038399-003
YS = .4254765-002 M.	.5104355-003
XS = -0.916 mm	
YS = 4.255 mm	

COEFFICIENTS OF RADIAL SYMMETRIC DISTORTION CURVE	
COEFFICIENT	STANDARD ERROR
K1 = -.8990007-002	.2113060-003
K2 = .4925623+000	.7570365-002
K3 = -.5390891+001	.8132587-001

COEFFICIENTS AND ORIENTATION OF DECENTERING DISTORTION CURVE	
COEFFICIENT	STANDARD ERROR
K4 = -.2029722-004	.7157778-005
K5 = -.9356722-004	.7316167-004
$\phi_T = \text{PHI-T} = -.1264493+002 \text{ g}$	.4194582+001 (GRADS)
	-11 22 49.585 (D.M.S) 13590.447 (SEC)

Table A.3 Variance-covariance Matrix of Mean Camera Calibration Parameters

(Report of Calibration by Stellar Method, 1983)

XP	YP	C	DELTA-X	DELTA-Y	K1	K2	K3	K4	K5	PHI-T
.1503-011	-.4030-013	-.1406-013	.4951-010	-.1943-011	.1320-012	.5634-011	-.1659-009	.7110-011	-.2459-010	-.2317-008
-.4030-013	.3952-012	.2694-015	.5856-012	.4394-010	.1501-011	-.4830-010	.4889-009	-.2508-012	.9313-012	-.2761-007
-.1406-013	.2684-015	.2766-012	.1795-011	-.1846-010	-.1028-009	.3317-008	-.3225-007	-.7662-013	.6605-012	.7053-009
.4951-010	.5856-012	.1775-011	.9222-007	.1374-007	.4098-008	.1889-008	-.2419-005	.1138-008	-.1429-007	-.1797-005
-.1943-011	.4394-010	-.1046-010	.1374-007	.2605-006	.5824-008	-.2737-008	.3444-005	-.3160-010	.9303-007	-.1993-004
.1374-007	.1501-011	-.1028-009	-.4098-008	.5824-008	.4465-007	-.1557-005	.1587-004	-.1980-010	.1062-009	-.5329-006
.5634-011	-.4830-010	.3217-008	.1889-008	-.2737-008	-.1557-005	.5731-004	-.6072-003	.0293-009	-.4482-008	.2301-004
-.1699-007	.4889-009	-.3225-007	-.2419-005	.3444-005	.1557-005	-.6072-003	.0614-002	-.1249-007	.6332-007	-.2844-003
.7110-011	-.2588-012	-.7662-013	.1138-008	-.3160-010	-.1780-010	.9293-009	-.1249-007	.5123-010	-.4003-008	-.9515-008
-.2459-010	.7313-012	.6605-012	-.1429-007	.9303-007	.1062-009	-.4482-008	.6332-007	-.4003-008	.5353-008	.4764-007
-.2317-008	-.2761-007	.7053-009	-.1797-005	-.1993-004	-.5329-006	.2301-004	-.2844-003	.9515-008	.4764-007	.4341-002

All parameters were determined in the fiducial coordinate system expressed in meters.

Calibration Temperature = 72<sup>o</sup>F

Calibration Atmospheric Pressure = 726 mb

Table A.4 Distortion Curve Data (Report of Calibration by Stellar Method, 1983)

MEAN DISTORTION CURVE DATA BASED ON COMBINING 4 PLATES

CALIBRATED FOCAL LENGTH = .3058822+000  
 TRANSFORMED FOCAL LENGTH = .3058914+000

CROSS-OVER POINT = .1741871+000  
 K-0 TERM = -.3010214-004

RADIAL DISTANCE (MM)	RADIAL SYMMETRIC CURVES				DECENTERED CURVE	
	COMPUTED DISTORTION (MICRONS)	MEAN ERROR (MICRONS)	TRANSFORMED DISTORTION (MICRONS)	MEAN ERROR (MICRONS)	DISTORTION (MICRONS)	MEAN ERROR (MICRONS)
2	.000	.000	-.060	.004	.000	.000
4	-.001	.000	-.121	.008	.000	.000
6	-.002	.000	-.183	.011	-.001	.000
8	-.005	.000	-.245	.015	-.001	.000
10	-.009	.000	-.310	.019	-.002	.001
12	-.015	.000	-.377	.022	-.003	.001
14	-.024	.001	-.446	.026	-.004	.001
16	-.037	.001	-.518	.029	-.005	.002
18	-.052	.001	-.593	.033	-.007	.002
20	-.070	.002	-.672	.036	-.008	.003
22	-.093	.002	-.755	.040	-.010	.003
24	-.120	.003	-.843	.043	-.012	.004
26	-.152	.004	-.935	.046	-.014	.005
28	-.189	.005	-1.032	.049	-.016	.006
30	-.231	.006	-1.134	.052	-.018	.006
32	-.278	.007	-1.242	.054	-.021	.007
34	-.331	.008	-1.355	.057	-.024	.008
36	-.390	.009	-1.474	.060	-.026	.009
38	-.455	.011	-1.599	.062	-.030	.010
40	-.526	.013	-1.730	.064	-.033	.011
42	-.603	.015	-1.867	.066	-.036	.012
44	-.686	.017	-2.011	.068	-.040	.014
46	-.776	.019	-2.161	.070	-.043	.015
48	-.872	.022	-2.317	.071	-.047	.016
50	-.974	.024	-2.479	.073	-.051	.018
52	-1.082	.027	-2.648	.074	-.056	.019
54	-1.197	.030	-2.822	.075	-.060	.020
56	-1.317	.033	-3.003	.076	-.065	.022
58	-1.443	.037	-3.189	.077	-.069	.023
60	-1.574	.040	-3.380	.078	-.074	.025

Table A.4 Distortion Curve Data(cont)

RADIAL DISTANCE (MM)	RADIAL SYMMETRIC CURVES				DECENTERED CURVE	
	COMPUTED DISTORTION (MICRONS)	MEAN ERROR (MICRONS)	TRANSFORMED DISTORTION (MICRONS)	MEAN ERROR (MICRONS)	DISTORTION (MICRONS)	MEAN ERROR (MICRONS)
62	-1.710	.044	-3.577	.070	-.079	.027
64	-1.852	.048	-3.770	.079	-.085	.028
66	-1.977	.052	-3.984	.079	-.090	.030
68	-2.147	.056	-4.194	.079	-.096	.032
70	-2.300	.061	-4.407	.079	-.102	.034
72	-2.457	.065	-4.624	.079	-.108	.036
74	-2.615	.070	-4.843	.078	-.114	.038
76	-2.776	.075	-5.064	.070	-.120	.040
78	-2.939	.080	-5.287	.079	-.127	.042
80	-3.102	.086	-5.510	.077	-.134	.044
82	-3.265	.091	-5.733	.076	-.141	.046
84	-3.428	.097	-5.956	.076	-.148	.048
86	-3.589	.103	-6.177	.075	-.155	.050
88	-3.747	.108	-6.396	.074	-.163	.052
90	-3.903	.114	-6.612	.073	-.171	.054
92	-4.055	.121	-6.824	.072	-.178	.057
94	-4.202	.127	-7.031	.071	-.187	.059
96	-4.343	.133	-7.232	.070	-.195	.061
98	-4.477	.139	-7.427	.069	-.204	.064
100	-4.603	.146	-7.614	.068	-.212	.066
102	-4.721	.152	-7.792	.067	-.221	.069
104	-4.829	.159	-7.960	.066	-.230	.071
106	-4.926	.165	-8.117	.065	-.240	.074
108	-5.011	.172	-8.262	.064	-.249	.076
110	-5.083	.179	-8.395	.063	-.259	.079
112	-5.141	.185	-8.513	.063	-.269	.081
114	-5.184	.192	-8.616	.062	-.280	.084
116	-5.211	.198	-8.702	.061	-.290	.087
118	-5.219	.205	-8.772	.060	-.301	.089
120	-5.210	.211	-8.822	.060	-.312	.092
122	-5.181	.218	-8.853	.059	-.323	.095
124	-5.131	.224	-8.863	.058	-.334	.097
126	-5.059	.230	-8.852	.057	-.346	.100
128	-4.964	.236	-8.817	.057	-.358	.103
130	-4.845	.242	-8.759	.056	-.370	.106
132	-4.702	.248	-8.675	.055	-.382	.109
134	-4.532	.254	-8.566	.054	-.395	.112

Table A.4 Distortion Curve Data(cont)

RADIAL DISTANCE (MM)	RADIAL SYMMETRIC CURVES				DECENTERED CURVE	
	COMPUTED DISTORTION (MICRONS)	MEAN ERROR (MICRONS)	TRANSFORMED DISTORTION (MICRONS)	MEAN ERROR (MICRONS)	DISTORTION (MICRONS)	MEAN ERROR (MICRONS)
136	-4.336	.259	-8.430	.053	-.407	.114
138	-4.112	.265	-8.266	.052	-.420	.117
140	-3.860	.270	-8.074	.050	-.434	.120
142	-3.579	.275	-7.853	.049	-.447	.123
144	-3.267	.280	-7.602	.047	-.461	.126
146	-2.925	.285	-7.320	.046	-.475	.129
148	-2.553	.289	-7.008	.044	-.489	.132
150	-2.146	.293	-6.663	.042	-.504	.135
152	-1.712	.290	-6.287	.039	-.519	.138
154	-1.244	.301	-5.879	.037	-.534	.141
156	-.743	.305	-5.439	.034	-.549	.144
158	-.210	.309	-4.966	.031	-.565	.147
160	.355	.312	-4.462	.028	-.581	.150
162	.952	.315	-3.925	.025	-.597	.153
164	1.580	.318	-3.357	.021	-.614	.156
166	2.239	.320	-2.758	.017	-.630	.159
168	2.929	.323	-2.128	.013	-.647	.162
170	3.640	.325	-1.469	.009	-.665	.165
172	4.395	.327	-.782	.005	-.682	.168
174	5.170	.329	-.068	.000	-.700	.171
176	5.970	.331	.672	.004	-.719	.174
178	6.792	.332	1.435	.009	-.737	.177
180	7.639	.334	2.221	.014	-.756	.180
182	8.505	.335	3.026	.019	-.775	.183
184	9.388	.337	3.849	.024	-.794	.186
186	10.286	.338	4.687	.029	-.814	.189
188	11.195	.339	5.536	.034	-.834	.192
190	12.112	.340	6.394	.040	-.855	.195
192	13.036	.341	7.257	.045	-.875	.199
194	13.961	.342	8.121	.050	-.896	.202
196	14.882	.343	8.982	.055	-.918	.205
198	15.795	.344	9.835	.060	-.940	.208



Table A.4 Distortion Curve Data(cont)

RADIAL DISTANCE (MM)	RADIAL SYMMETRIC CURVES				DECENTERED CURVE	
	COMPUTED DISTORTION (MICRONS)	MEAN ERROR (MICRONS)	TRANSFORMED DISTORTION (MICRONS)	MEAN ERROR (MICRONS)	DISTORTION (MICRONS)	MEAN ERROR (MICRONS)
200	16.696	.345	10.676	.065	-.962	.211
202	17.500	.347	11.499	.069	-.984	.214
204	18.440	.348	12.299	.074	-1.007	.217
206	19.270	.350	13.069	.078	-1.030	.220
208	20.065	.352	13.803	.083	-1.053	.223
210	20.816	.355	14.495	.087	-1.077	.226
212	21.517	.358	15.136	.092	-1.101	.229
214	22.161	.362	15.719	.096	-1.126	.233
216	22.737	.366	16.235	.101	-1.151	.236
218	23.230	.372	16.676	.107	-1.176	.239
220	23.655	.378	17.032	.113	-1.202	.242
222	23.977	.386	17.294	.121	-1.228	.245
224	24.193	.395	17.450	.130	-1.254	.249
226	24.293	.406	17.490	.141	-1.281	.252
228	24.266	.419	17.403	.154	-1.308	.255
230	24.090	.434	17.175	.169	-1.336	.258
232	23.777	.452	16.793	.197	-1.364	.262
234	23.209	.473	16.246	.208	-1.392	.265
236	22.621	.497	15.517	.233	-1.421	.269
238	21.756	.525	14.592	.261	-1.450	.272
240	20.679	.556	13.455	.293	-1.480	.276
242	19.374	.592	12.090	.329	-1.510	.279
244	17.824	.632	10.479	.370	-1.540	.283
246	16.010	.676	8.605	.415	-1.571	.286
248	13.914	.726	6.448	.465	-1.602	.290
250	11.515	.781	3.990	.520	-1.634	.294
252	8.794	.842	1.208	.580	-1.666	.298
254	5.728	.909	-1.918	.646	-1.699	.302
256	2.296	.982	-5.410	.719	-1.732	.306
258	-1.526	1.062	-9.293	.797	-1.766	.310
260	-5.762	1.148	-13.589	.883	-1.800	.314

Large Format Camera zenith. Figure A.6 shows the star images measured on each of the four plates.

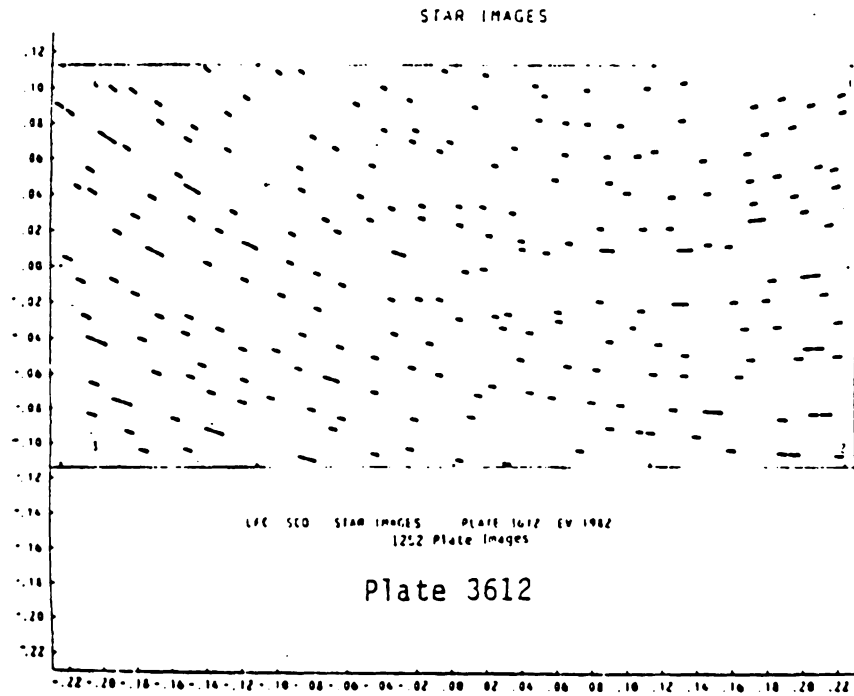
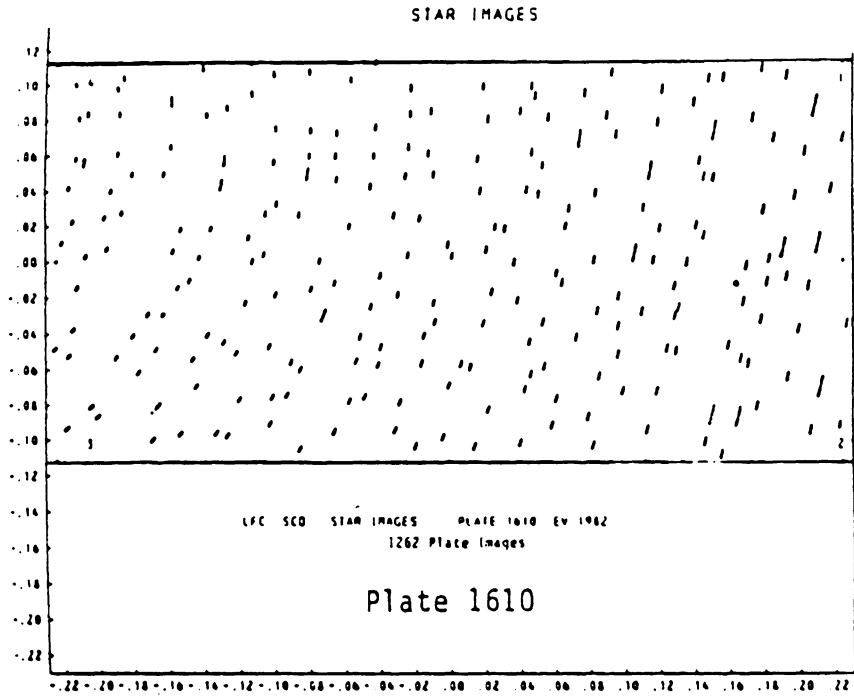


Figure A.6 Star Images Measured on Each Plate  
(Report of Calibration by Stellar Method, 1983)

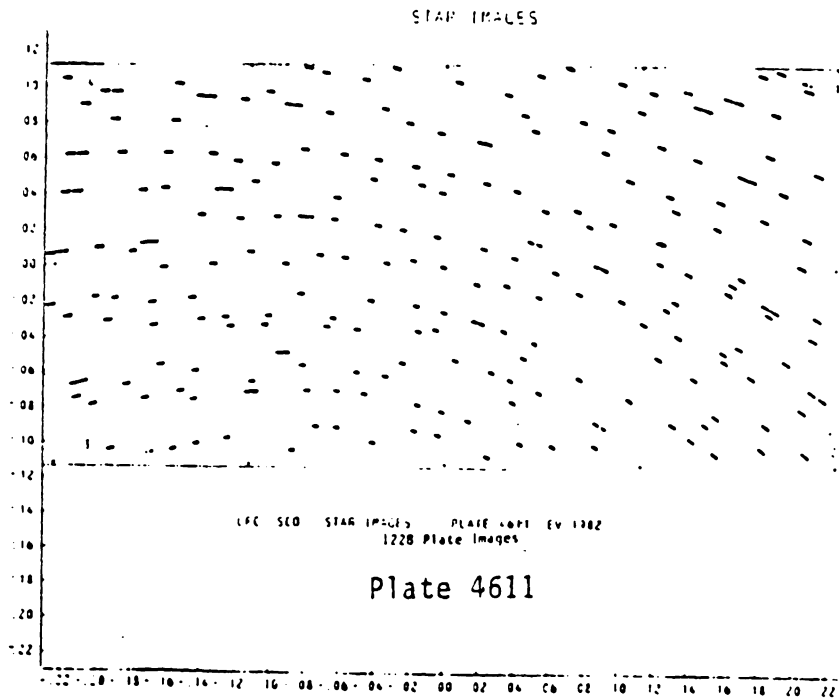
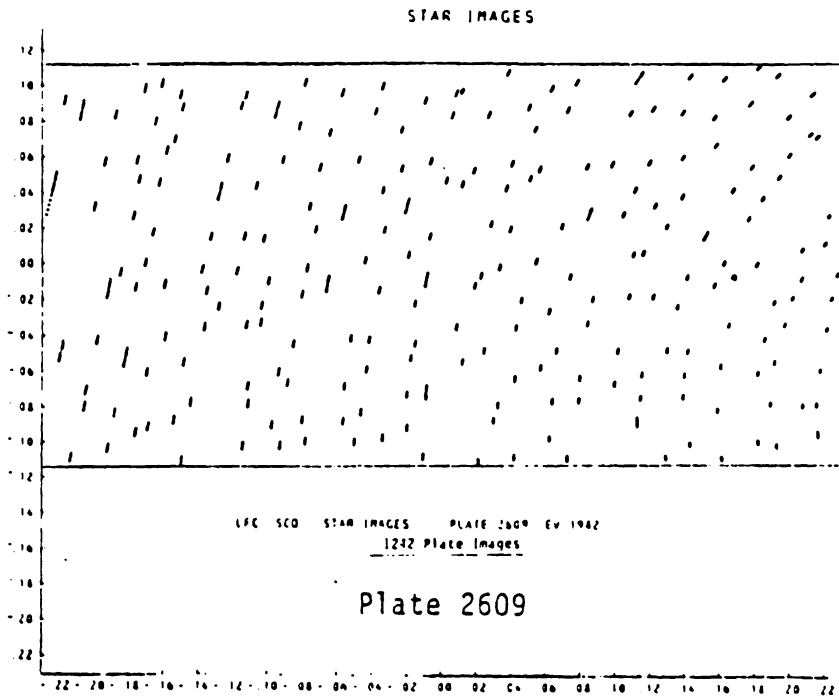


Figure A.6 Star Images Measured on Each Plate(cont)

**The vita has been removed from  
the scanned document**